

Volcaniclastic Aggradation in El Tarr Area, Southeastern Sinai, Egypt: Petrological and Geochemical Evidence

EZZ EL DIN ABDEL HAKIM KHALAF

Geology Department, Faculty of Science, Cairo University

Received: 24/3/2003 Revised: 29/3/2004 Accepted: 8/5/2004

ABSTRACT. The Tarr complex forms the southernmost portion of the Kid Group in the Southeast Sinai Peninsula. This complex consists of diverse interstratified volcanic and volcaniclastic sedimentary strata and cogenetic hypabyssal intrusive rocks of Late Proterozoic age. The occurrence of slightly preserved glass shards and volcanic clasts within volcaniclastic sediments indicate a narrow time span between eruption and final deposition by resedimentation. The volcano-sedimentary sequence of El Tarr area displays a low metamorphic grade and is nearly undeformed. These volcaniclastic rocks are characterized by rapid lateral and vertical facies and petrofacies variation. Modal analysis of these rocks defines a source area comprising mainly volcanic and intrusive rocks, with no indication of continental detritus or detritus from exotic sources.

The studied sequence is divided into three stratigraphic intervals on the basis of the predominant lithosomes in each of the intervals. The lowermost stratigraphic interval contains metamorphosed felsic pyroclastic rocks with marble intercalations, continues vertically to mafic and intermediate volcanic flows, pyroclastic fall and flow deposits and local interbeds of clast-supported conglomerates, associated with cross-laminated sandstones with lensoidal layers of tuffaceous mudstones. These rocks were deposited in a low relief, proximal alluvial fan volcanic apron environment. The middle stratigraphic interval consists of thick massive to bedded coarse to medium-grained sandstones and interbeds of tuffaceous mud/siltstones, with lensoidal beds of metamorphosed mafic volcanics. Rocks in the middle interval were deposited in distal alluvial fan volcanic apron environment. The upper stratigraphic interval contains matrix/clast-supported conglomerates of mixed sources that were deposited in poorly confined, shallow proximal braided river channels on a fluvial plain.

Tectonics are perceived to be a major control on the positioning and long-term evolution of alluvial systems. By increasing slope gradients through uplift and tilting, or by changing local base-level, incision can be stimulated leading to a switch in the active area of sedimentation. The switch from alluvial fan to braided river sedimentation and the spatially variable patterns of incision into the alluvial fan bodies can be accounted for by a phase of deformation which affected the El Tarr volcaniclastic rocks during Late Proterozoic time. A lack of pedogenic modification throughout most of the channelized sediments suggests high rates of sedimentation which inhibited soil development. The whole studied sequence is similar to rock units in arc-flank volcanic complexes which are interpreted to have accumulated principally on river flood plain and alluvial fan and local aeolian environment.

Introduction

Geologic research in the past decade has focused on the relationships between volcanism and sedimentation (*e.g.* Fisher and Smith, 1991). These relationships are important for better understanding for several reasons. The most significant aspect of volcanic hazards is the catastrophic sedimentary processes accompanying and succeeding eruptions. Such processes include debris flows, hyperconcentrated flows, aggradation of drainage basins, and general disruption of the hydrologic system in the region surrounding the active volcano. These hazards may continue for decades after a large explosive eruption. A second reason for studying sedimentation in volcanic terrains is that volcaniclastic rocks are often important components of sedimentary basins and can provide useful information on basin evolution (Fisher, 1984). Finally, most subaerial volcanoes form topographic highs that are subsequently eroded away and reworked by normal surface processes to form volcaniclastic fluvial, lacustrine and aeolian deposits. Even in these well-preserved young systems, where the relationships between volcaniclastic deposits and a volcanic vent are clear, careful documentation of facies characteristics is required to distinguish between primary deposits and their reworked equivalents (Smith and Katzman, 1991). Thus, much of the record of volcanism on Earth is recorded in sedimentary successions.

Volcaniclastic layers (VLs) have been extensively investigated in recent years (Fisher and Schmincke, 1984; Cas and Wright, 1987; Cas and Busby Spera, 1991), since they are the best means available to stratigraphers for long-range physical and geochronological correlations (Calanchi *et al.*, 1998). Moreover, they provide information about past volcanic activity. Most of the preserved ancient VLs, however, were deposited in a marine environment, where the interaction between volcanic and sedimentary processes may produce a

strong convergence of lithofacies among volcanic products of distinct origin, thus hindering their correct interpretation. For example, primary pyroclastic products as ash falls, pyroclastic flow and surge deposits may macroscopically resemble pyroclast-rich detrital sediments that result from epiclastic processes involving freshly erupted pyroclasts (Cas and Wright, 1987).

The Tarr area (long. 34°21'30" - 34°18'30", and lat. 28°13'30" - 28°11'5") covers an area of about 36 km², near the Gulf of Aqaba. It comprises the southernmost portion of the Kid Group in the Southeast Sinai Peninsula. The study area consists of a number of distinct complex tectonic blocks with rocks of different petrologic classes. It includes all of the volcano-sedimentary units along the Southern wadi Kid region. The geologic evolution of Kid area was previously reviewed by many authors (Shimron, 1980, 1983; Reymer, *et al.*, 1984; Furnes *et al.*, 1985; EL Gaby *et al.*, 1991). Previous works on the stratigraphy and composition of the volcaniclastic rocks are rather limited. So, the main purposes of the present investigation are : (a) to document their composition, distribution and sedimentology; (b) to distinguish between the volcanic and sedimentary processes that gave origin to these deposits; (c) to suggest a depositional model for volcaniclastic deposits in the study area.

Geological Background

Wadi Kid area, Southeast Sinai is largely occupied by a volcano-sedimentary succession intruded by gabbro, granodiorite, younger granite and minor albitite intrusions. These rocks form a part of the Arabian-Nubian Shield, which extends over most of NE Africa and Arabia. Moreover, the investigated area is cross-cut by swarms of mafic and felsic dykes trending in NE-SW direction.

The Kid Group forms a roughly domal structure about 30 × 30 km² that comprises four geotectonic formations including Umm Zariq Fm., Malhag Fm., Heib Fm. and Tarr Fm. (Fig. 1). The Umm Zariq Fm. is a metasedimentary sequence, mainly formed by metapelites with some metapsammites. The schistose metapelites consist of biotite, muscovite, retrograde chlorite and feldspar along with porphyroblasts of garnet, andalusite, and cordierite, indicating amphibolite facies of the low-pressure/high temperature (LP/HT) type. The Malhag Fm. is a metavolcanic sequence (Furnes *et al.*, 1985) containing mainly schists and minor non-schistose massive equivalents. The schistose metavolcanics consist of feldspar, quartz, biotite and hornblende, indicating upper-amphibolite facies. The Heib Fm. is a mixed sequence of metasediments and metavolcanics. Rhyolitic and andesitic volcanics can be recognized. The Tarr Fm. recorded in the southern parts of the wadi Kid, is dominantly a sedimentary and volcanic sequence. These rocks display a lower metamorphic grade than the Umm Zarig and Malhag Fms. and are less deformed. In spite of this, sedi-

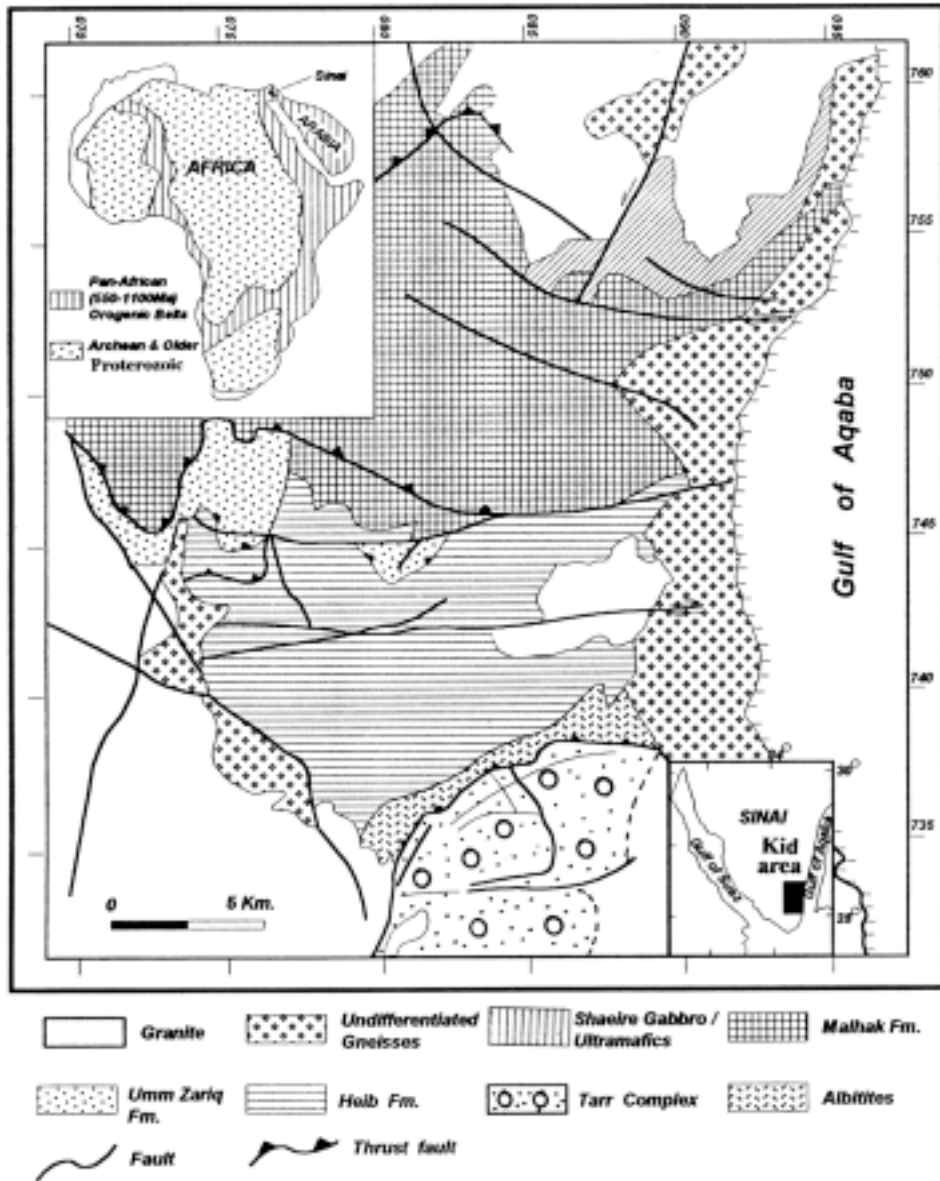


FIG. 1. Generalized geology of the Kid Group (after Shimron, 1980).

mentary and volcanic structures and textures are generally unaffected, and delicate macro/microscopic features such as glass shards, porphyritic fabric, cross-lamination and fining-upward sequence are excellently preserved.

Metamorphic grades of the El Kid area range from lower-greenschist to amphibolite facies with a general trend of increase towards the central and northern parts of the area. Lower-greenschist facies rocks dominate the southern areas. Reymmer *et al.*, (1984) calculated a temperature of 700°C and a pressure of 3 to 4 kbar for the Malhag and Umm Zariq Fms. in the central wadi Kid. Temperatures of 300°C and pressures of 2.0 kbar have been deduced for the lower-greenschist facies rocks in the southeastern part of the complex.

Geochronologically, it can be concluded that deposition of sediments and volcanics took place between 770 Ma and 650 Ma ago (Priem *et al.*, 1984), when the metamorphism started. The main amphibolite phase of metamorphism started at about 620 Ma ago. Pulses of metamorphism and the intrusion of granites continued till the early Cambrian and were accompanied by the intrusion of dykes (Ayalon *et al.*, 1987).

Facies Stratigraphy

The Tarr area which occupies the southern part of wadi Kid area, is composed of moderately indurated volcaniclastic deposits, including volcanics, pyroclastics, epiclastics, albitite and other intrusive rocks (Fig. 2). The whole succession is folded into a series of anticlines and synclines trending ENE-WSW. It was also subjected to low-pressure metamorphism in several aureoles (Reymmer *et al.*, 1984) reaching up to the development of diatexites in some aureoles. The investigated rock units have been divided into three stratigraphic intervals on the basis of the colour, sedimentology and predominant lithosomes in each of the intervals. The stratigraphic boundary among the three intervals can be either a marked disconformity or an intercalated contact. All three intervals display moderate to substantial lateral changes in the relative abundances and vertical arrangement of their constituent lithosomes (Figs. 3A/B), a characteristic common to subaerial volcanic arcs (cf. Cas and Wright, 1987).

Lower Interval

The lower interval, which ranges in thickness from 50 to 100 m, is composed in stratigraphic upward order of metamorphosed pyroclastic rocks with marble intercalations, volcanic and pyroclastic rocks (~ 70%), conglomerates, sandstones and locally interbedded tuffaceous mudstones. This interval is best exposed around wadi Kid and at the entrance of El Tarr. Everywhere in the lower interval, reworked deposits are subordinate to volcanics and pyroclastics.

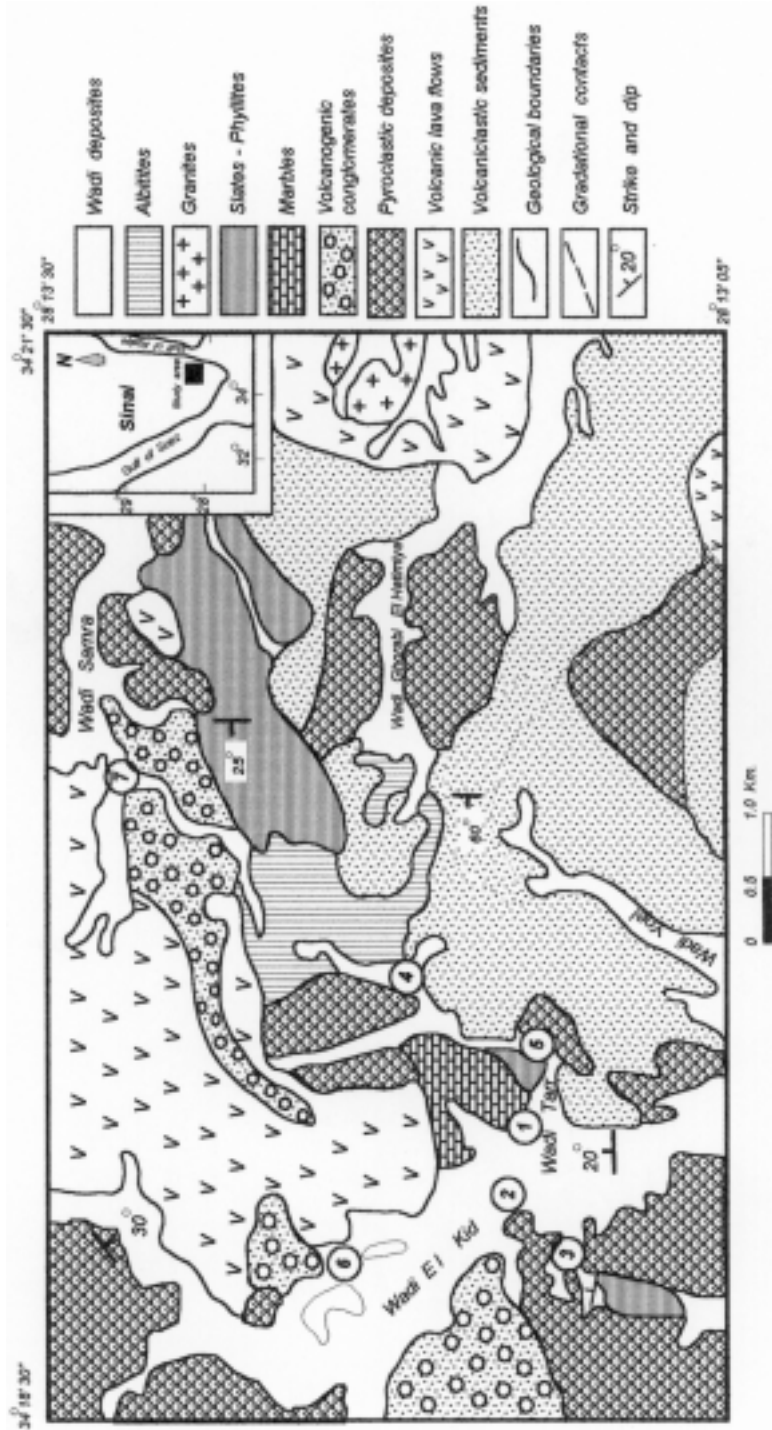


Fig. 2. Geological map of the El Tarr area.

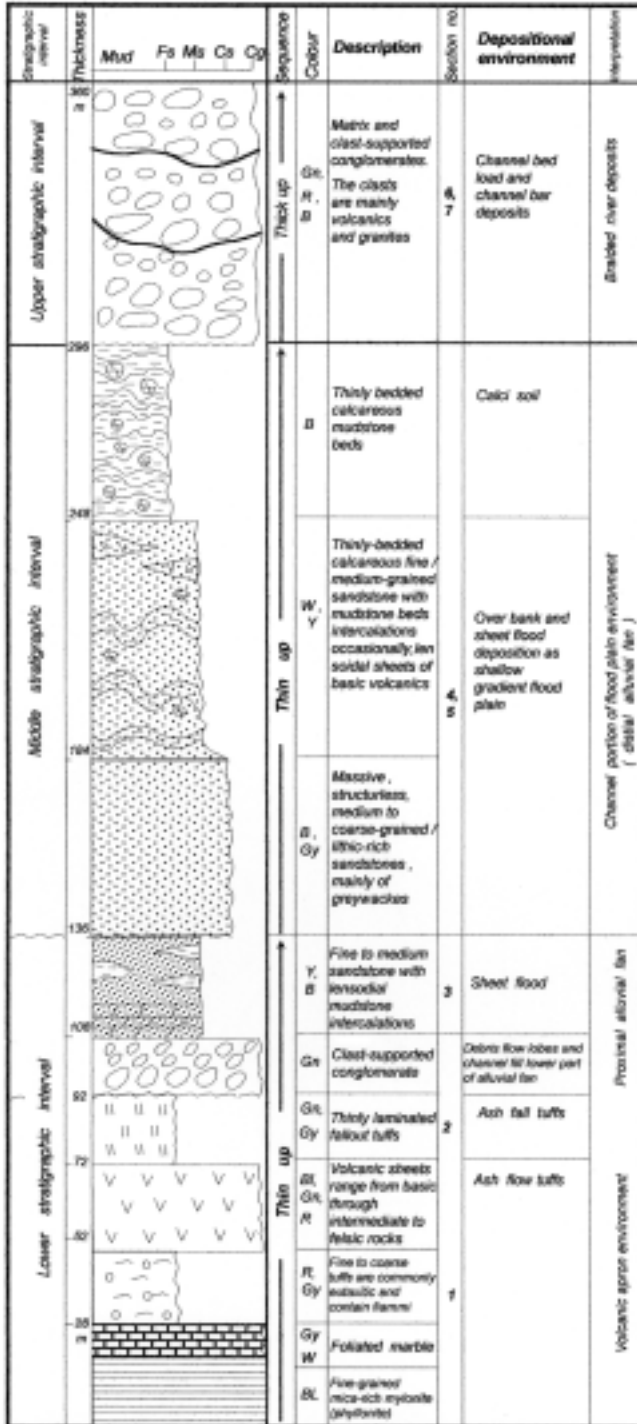


Fig. 3A. Stratigraphic sections and depositional environments for the volcaniclastic rocks exposed at the study area. See Fig. (2) for location and Fig. (3B) for legend.



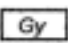


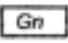


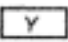
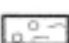

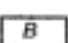








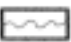
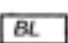
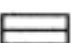
Lithology	Sedimentary structures	Colour
 Dynamic metamorphosed rocks	 Lamination	 Grey
 Marble	 Wavy lamination	 Green
 Volcanic flows	 Cross lamination	 Yellow
 Crystal-phynic welded tuffs	 Imbrication	 Brown
 Laminated tuffs	 Graded bedding	 Red
 Conglomerate	 Carbonate nodules	 White
 Sandstone	Basal contacts	
 Mudstone	 Erosional surface	 Black
	 Abrupt	
	<i>Thin-up</i> → <i>thinning up ward</i>	
	<i>Thick-up</i> → <i>thickening up ward</i>	

FIG. 3B. Symbols used in the measured stratigraphic sections (Fig. 3A).

Metamorphosed Felsic Rocks

These rocks are well exposed at the entrance of El Tarr area. In the field, they can be recognized by their fine grain size and strongly developed, usually regular and planar foliation. The predominant constituent minerals are biotite, muscovite, chlorite and quartz with feldspar porphyroclasts. The feldspar porphyroclasts suffer slight alteration to kaolinite and exhibit undulose extinction and granulation especially along grain boundaries (Fig. 4A). The foliation in the quartz-mica-rich matrix wraps around feldspar porphyroclasts. The constituents of the matrix are thought to be derived from coarse-grained parent rocks, by intracrystalline deformation and recrystallization. The variety of grain size, undulose extinction and granulation of strained porphyroclasts prove that these rocks have undergone dynamic metamorphism and were derived from felsic py-

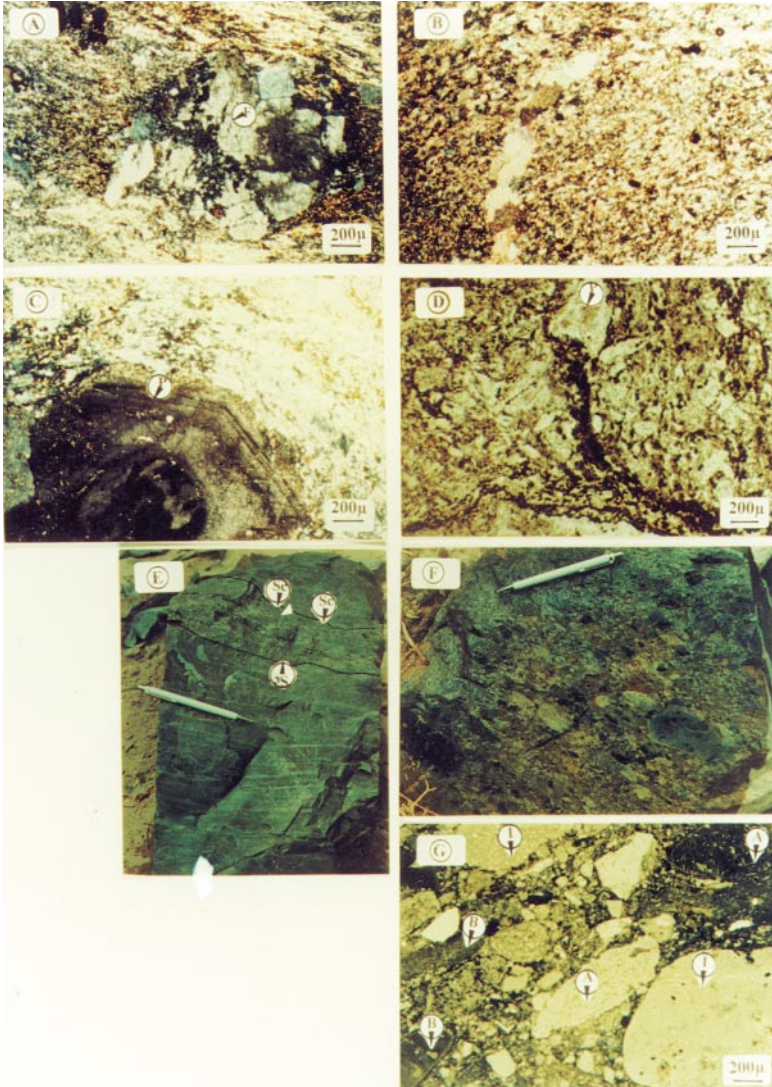


FIG. 4. A. Strained feldspar porphyroclast (F) with undulose extinction and fragmentation along crystal borders set in mica-rich planar foliated matrix.
 4B. Thinly-bedded calcite with siliceous argillite intercalation.
 4C. Oscillatory-zoned plagioclase phenocryst (P) embedded in fine-grained groundmass with pilotaxitic and trachytic texture.
 4D. Plagioclase phenocryst (P) set in a matrix composed of abundant welded sinuously curved glass shards forming fiamme.
 4E. Thinly-bedded fine-grained fallout tuff with scouring upper surface (Sc).
 4F. Oligomict conglomerate exhibit graded bedding and imbrication.
 4G. Photomicrograph shows framework-supported that is mainly composed of volcanic clasts {basaltic (B), andesitic (A) and ignimbritic (I) rock types}.

roclastic predecessor. These rocks have been classified as phyllonite based on the fabric and matrix-porphyroclast ratio. Some authors use the term phyllonite as a synonym for ultramylonite (*e.g.* Passchier and Trouw, 1996).

Metamorphosed pelitic sediments including garnet, staurolite, andalusite and coridierite in schists and gneisses appear only in the central wadi Kid area, where the metamorphic grade reaches the amphibolite facies. Near the contact with granodiorites-granites, these pelitic rocks contain randomly oriented, euhedral staurolite, and (or) andalusite crystals.

Marble

Marble units, are thinly and uniformly bedded (Fig. 4B) and have siliceous argillite intercalations. Based on its uniformity and fabric, these units are considered as metamorphosed calcareous rocks.

Volcanic Lava Flows

These rocks unconformably overlie the metamorphosed and ignimbritic rocks. They occur as individual massive sheets 3 to 8 m thick, more commonly as sequences of sheets up to 25 m thick. Both are broadly lensoidal, and typically extend laterally. The volcanic rocks range in composition from basic and intermediate to felsic rocks, with epiclastic sediment intercalations.

Petrographically, the basic rocks are medium-grained, nonporphyritic and greenish grey in colour. They encompass tabular altered plagioclase and ferromagnesian minerals which are completely replaced by anhedral clots of chlorite, epidote, ziosite, calcite and opaques. The intermediate rocks are porphyritic, fine-medium grained and essentially composed of zoned plagioclase and green hornblende embedded in pilotaxitic and trachyritic matrix composed of plagioclase laths, actinolite, opaques, epidote and occasionally quartz microporphyritic crystals (Fig. 4C). The felsic rocks are fine-grained and composed of plagioclase (An₁₅) and resorbed quartz phenocrysts dispersed in a felsitic groundmass of feldspar microlaths, quartz, biotite and opaques.

Pyroclastic Rocks

These rocks include both welded ignimbrites and thinly bedded tuffs. Ignimbrites, which underlie the volcanics comprise monotonous massive, densely welded eutaxitic tuffs. They are fine-grained, light grey in colour and composed of quartz, plagioclase, rare rock fragments and abundant welded sinuously curved glass shards or fiamme showing preferred orientation (Fig. 4D). The glass shards exhibit partial devitrification to quartz, sericite and clay minerals. Eutaxitic fabrics show pronounced flattening and pinching and molding around

lithic and crystal fragments. These stratified lithofacies were dominantly produced by coalesced non-particulate (rheomorphic) flow (Branney and Kokelaar, 1992), and the sheets closely resemble lava. The general absence of vesicles and lithophysal cavities in these deposits indicate substantial degassing before emplacement, although the stratification itself probably reflects segregation of remaining volatiles. So, these ignimbritic sheets are interpreted as lava-like ignimbrites that were deposited rapidly from a large-volume pyroclastic density current directed laterally from a fountain during catastrophic venting from fissures.

The bedded tuffs which overlie the volcanics, range in size from dust to lapilli; agglomerates are rare. They comprise crystal and lithic tuffs with crystal ashes. The rock fragments are dominantly of andesite and dacite and rare basaltic fragments. The upper part of these tuffs is cut by low-angle scour surface (Fig. 4E) that is draped by steeply dipping laminated tuffs, which locally show evidence of slumping. These structures are interpreted as up-current facing scours that were eroded by pyroclastic currents and plastered with damp ash (Moore and Kokelaar, 1998). These tuff successions accumulated from distal low-concentration pyroclastic density current and by pyroclastic fallout during a phreatomagmatic eruption. The phreatomagmatism inferred from the abundance of fine-grained tuffs, and the occurrence of steep stratification indicative of plastering of wet ash, is considered to have been caused by the interaction of magma with groundwater. Its pyroclastic eruption origin is indicated by its apparently degassed state on emplacement, the absence of brecciated lateral margins (Bonnichsen and Kauffman, 1987), and the presence of stratified eutaxitic tuffs.

Crudely Stratified Conglomerates

This facies is dominated by crudely horizontally stratified beds which occur as thin discontinuous beds or as stacked lenses. It is composed of clast-supported pebbly conglomerates displaying moderate to poorly sorting and disorganized fabric. Horizontal stratification is distinguished by fine sandstone layers or by zones with developed imbrications of pebbles (Fig. 4F). Their contacts are planar or slightly irregular. The clasts are mostly volcanic in composition embedded in sandy to sandy-muddy matrix (Fig. 4G).

The deposition of crude conglomerate layers resulted from poorly confined sheet flows where normal grain-by-grain tractional bed load sedimentation predominated and a traction carpet was not developed (Hartley, 1993). These thin conglomerate layers were formed during discharge fluctuations. They were interpreted in terms of longitudinal gravel bars associated with fluvial channels collectively forming broad, low relief bar complex (Olson and Larsen, 1993).

Cross-Laminated Sandstones

This facies is composed of yellowish-reddish brown, medium-grained moderately to poorly sorted sandstones, with lensoidal clay intercalations (Fig. 5A). They reveal small-scale cross-laminating sets. Horizontal and inclined laminations are present. They are basically composed of subrounded, monocrystalline quartz grains which range in size between medium silt and medium sand (~ 20%, by volume), dominant feldspar (30-50%) and lithic fragments (~ 30%). Feldspar grains are almost all plagioclase (albite/oligoclase) and rounded to subrounded (Fig. 5B). Lithic fragments are mainly volcanic with subordinate argillaceous and siliceous (chert) rock fragments. These volcanic grains exhibit trachytic and often hyalopilitic, pilotaxitic and vitric textures, which now are slightly to completely replaced by aggregates of fine granular epidote. All the constituents are embedded in sand-rich matrix composed of fine-grained quartz, mica flakes, opaques, epidote and clay.

The planer cross-laminated sands are formed on higher topographic elevations as bar-top sheets, or deposited as wedges at bar margins by surface runoff (Miall, 1996). An alternative origin for these deposits as wind blown sand cannot be ruled out. The presence of such sands on these gravel sheets, in this facies points to their deposition during waning flood flows as a result of direct fall out sedimentation (Jo *et al.*, 1997).

Interpretation: the lower interval accumulated during a time of abundant volcanic activity interspersed with episodes of erosion and sedimentary deposition by fluvial, less-common debris-flows and rare eolian processes. These rocks in the lower interval were deposited in a low relief, proximal volcanic fan apron environment.

Middle Interval

The middle interval which ranges in thickness from 100 to 150 m, is composed predominantly of epiclastic rocks (~ 90% of interval) including medium to fine-grained sandstones (MSS/FSS) and silt/mudstones (M) with basic volcanics (V) intercalations locally (Figs. 3 & 5C). This interval is recorded in El Tarr area itself.

Sandstone Facies Associations

Massive Sandstones

This facies forms the basal part of the interval. It is characterized by massive, blackish grey, fine to coarse-grained sandstones which occur as 2.0-3.0 m thick beds and lack internal stratification. These rocks are poorly sorted, quartz-poor and are dominantly composed of feldspar and rock fragments. Quartz grains form less than 10%, and are always monocrystalline, anhedral, angular and has

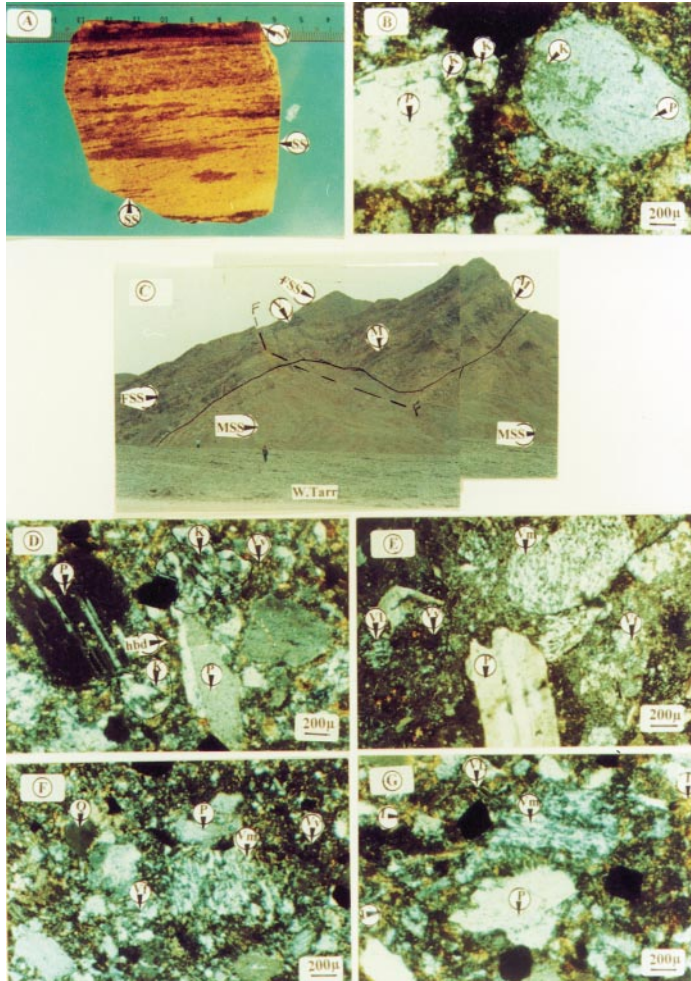


FIG. 5A. Polished slab of medium-grained sandstone (SS) showing planar/low-angle cross-lamination with lensoidal mud layers intercalations (M).
 5B. Rounded to subrounded plagioclase (P) exhibit partial alteration to kaolinite (K) along crystal margins with pore-filling fine crystalline kaolinite booklets (K).
 5C. Faulting and tilting of bedded volcaniclastic sediments (middle interval) observed at the mouth of wadi EL Tarr.
 5D. Twinned plagioclase (P), hornblende grains (hbd), volcanic fragments with vitric texture (Vv) and pore-filling coarse crystalline kaolinite booklets (K) in between feldspar grains in poorly-sorted sandstone.
 5E. Massive sandstone contains mainly volcanic fragments with lathwork (VL), microlitic (Vm), felsitic (Vf) and vitric textures (Vv); most crystal grains are plagioclase (P).
 5F. Poorly-sorted massive sandstone encompasses volcanic clasts with microlitic (Vm), vitric (Vv) and felsitic texture (Vf), quartz (Q) and plagioclase grains (P).
 5G. Plagioclase (P), volcanic clasts with microlitic (Vm), lathwork (VL), and vitric texture (Vv) and diagenetic illite-like hair (I), most probably after mica.

uniform sharp extinction (non-undulose), some of which exhibit bibyramidal crystal forms diagnostic of volcanic origin. Polycrystalline quartz grains are mainly chert. Feldspar grains are almost all plagioclase which exhibit albitic twinning (Fig. 5D) and occasionally oscillatory zoning. The lithic fragments are mainly volcanic clasts which constitute 50 to 70% of the whole rocks and contain plagioclase and altered mafic phases set in a matrix of fine quartz, chlorite and epidote. These lithic clasts exhibit mainly lathwork and often microlitic and felsitic textures (Figs. 5E/F). Detrital mica flakes are common and diagenetically altered to hairy illite (Fig. 5G). The overall dominance of volcanic grains of lathwork to microlitic textures, together with the common occurrence of plagioclase and mafic grains and trace amount of quartz clearly suggest the dominance of basaltic to andesitic rocks in the source terrain. The ratio of plagioclase to total feldspar grains (P/F) averages 0.94 for these sandstones, reflecting an extreme lack of K-feldspar. The detrital mode ($Q_{<10}F_{30}L_{70}$), P/F (0.94) and Lv/L (0.94) ratios of the sandstone suites are similar to those of most modern and ancient volcanic arc sands (Dickinson and Suczek, 1979).

Bedded Fine to Medium-grained Calcareous Sandstones

This facies is represented by apparently massive, yellowish white sandstone, which is generally fine to medium-grained in size. It has an erosive sharp base and internal erosional surface as well. It is interbedded with thinner silt and silty-mudstone beds (Fig. 6A). Occasionally, mudstone layers overlie fine-grained sandstone. This facies is basically composed of quartz, feldspar, mafic clasts and volcanic lithic clasts (Fig. 6B). All the constituents are set in calcareous cement, which shows partial to complete replacement of quartz and feldspar grains.

The large lateral extent, little thickness variation, dominance of horizontal laminae (stratification) together with their grain size variations suggest that the thick sandstones represent deposition by sheet flood events under an upper flow regime. Besides, the close association of this facies with mudstone beds and their deposition under an upper flow regime indicate distal sheet floods at the toes of alluvial fans in a lacustrine environment. Moreover, the interbedded mud-rich and sand-rich units are indicative of changes of the alluvial depositional style. The sand beds point to waning flows and deposition from density underflow occurring during flood-related influxes and sediments (Massari *et al.*, 1993). The mud drapes reflect falling out of suspension during low flow periods in the deepest parts of channels and from weak traction currents.

Calcareous Tuffaceous Silt/Mudstone Facies Association

This facies occurs either as layers intercalated with sandstones or homogeneous stacks capping the sandstones (Fig. 6C). In outcrop, they are light yel-



- FIG. 6A. Handspecimen shows rhythmic intercalations of fine/medium-grained sandstone (light colour) and mudstone layers (dark colour) with parallel and wavy lamination.
- 6B. Framework-supported sandstone contains quartz (Q), plagioclase (P), volcanic clasts with vitric texture (Vv) and pore-filling coarse booklets of kaolinite (K) set in calcareous cement.
- 6C. Thinly-laminated mudstone (M) with wavy lamination overlies thinly-bedded fine-grained sandstone (SS).
- 6D. Parallel, wavy and convolute laminations in mudstone. Notice the presence of rip-up mud clasts (RU).
- 6E. SEM image shows skeletal form of feldspar after near complete dissolution.
- 6F. Calcite nodules (Cc) with different morphology in mudstone.
- 6G/K. Chlorite pseudomorphs, most probably after amphibole (6G) and pyroxene (6K).

low to brown and occasionally red in color and moderately to poorly sorted. As the topography is subdued upsection, the beds become thicker and more laterally persistent. Wavy-planar to low-angle truncating lamination and convolute structures are the dominant fabrics present in this facies (Fig. 6D). The lamination is defined by vertical grain size changes, especially coarse-grained trains of a few millimeters to a few centimeters in thickness within fine to medium-grained matrix. These coarse-grained trains generally have sharp, well-defined margins. The occasional presence of rip-up mud clasts (RU) reflect great discharge fluctuations and reworking of mudstone laminae (Fig. 6D).

Petrographically, this facies reveals a closed to locally open framework of quartz, feldspar, vitric lithic fragments, carbonate nodules, epidote and chlorite pseudomorphs. Quartz grains occur as subrounded, monocrystalline grains of medium silt to fine sand size. They are subangular and exhibit low sphericity and poor sorting as well as open packed fabric. The feldspar are partially to completely altered to kaolinite, sericite and minor chlorite. Selective feldspar dissolution as evidenced by skeletal remnants of partially to completely, dissolved feldspar grains may be related to the processes of kaolinitization (Fig. 6E). The dissolution of feldspar grains may be explained by their relative instability in acidic conditions (Surdam *et al.*, 1984). Carbonate nodules occur as pore-filling and grain-replacive cement phases. They replace detrital grains (mainly feldspar) and corrode quartz grain margins. Poikilotopic sparry calcite grains have a patchy distribution and are either dispersed in the surrounding matrix or as stacked grains. These calcite grains occur in different forms, as cryptocrystals intermixed with clays, large rhombic crystals or xenotopic crystals (Fig. 6F); that range in diameter between 1.0-3.0 cm. Chlorite occur occasionally as euhedral pseudomorphs, most probably after pyroxene/or amphibole (Figs. 6G/K). The fine-grained matrix appears to have been vitric, but it has been completely replaced by a mosaic of quartz, chlorite, sericite, epidote and disseminated iron oxides.

Interpretation: rocks in the middle interval were deposited in a low-relief distal alluvial fan/volcanic apron environment. The facies association of this interval is interpreted as flood plain deposits based on color, grain size, common occurrence of carbonate nodules and the vertical fining-up texture with the increase in distance from the channel. The flood plain development points to an inactive period of alluvial system which received sediments during over-bank flooding that have been subjected to pedogenic processes (Jo *et al.*, 1997). The sheet-like geometry of the over-bank fines with lenses of fine sand indicates their origin by vertical aggradation (Miall, 1985).

In summary, low-gradient flood plain environments, represented by laterally extensive intervals of sandstones and mudstones, prevailed across much of the

region when the middle interval began to accumulate and continued to exist throughout deposition of most of the El Tarr exposure. Local, low-volume eruptions of lava flows occurred episodically during renewed magmatic activity as the middle interval was being deposited.

Upper Interval

The upper interval is dominated by heterolithic conglomerates that are interbedded with subordinate sandstone and siltstone units. Individual conglomeratic units can often be traced laterally over several tens of metres with a sheet-like geometry. Two types of conglomerates are identified on the basis of their sedimentary fabrics: (1) Matrix-supported conglomerates and (2) Clast-supported conglomerates.

Matrix-supported conglomerates typically occur as massive units 1-3 m in thickness. They lack any internal structure and comprise very poorly sorted pebble to cobble size clasts-supported within a muddy sand matrix (Fig. 7A). The clasts are rounded to sub-rounded and show no preferred orientation.

Clast-supported conglomerates typically occur as crudely stratified units. These conglomerates often display a weak horizontal fabric on a decimeter scale and comprise poor to moderately sorted gravel to boulder size clasts (Fig. 7B). The clasts are angular to sub-rounded and show no imbrication.

The conglomerate outcrop mainly occurs around wadi Kid, and at the central and northeast of wadi Tarr in low relief. The clast types are mainly basaltic and andesitic porphyries, ignimbrite, tonalite, granodiorite, proper granite and epiclastic rocks (Fig. 7C). The variation of these clast in composition is considered to correspond to variations of the exposed rock types in the study area. Along the central portions of wadi Tarr (wadi Hatimiya in particular), the clasts of these conglomerates comprise gabbro and plagiogranite (albitite). Towards the northeast (wadi Samra) increasing amounts of soda granite and granophyre are recorded, occasionally comprising up to 30-40% of some conglomeratic beds. So, the presence of granodioritic, granitic, gabbroic and albititic pebbles suggests that these conglomerates represent a younger interval than that of the rocks in the lower and middle intervals.

Matrix-supported, poorly sorted disorganized conglomerates suggest deposition from sediment gravity processes such as cohesive debris flows. The clast-supported conglomerates point to viscous cohesionless debris flow and usually indicate high energy flow transporting coarse bed load. The improved sorting and the presence of an internal structure within the clast-supported conglomerates indicates deposition from fluid-gravity flows (Costa, 1988). The laterally unconfined nature of these flows suggests a sheetflooding process (Blair, 1987; Well and Harvey, 1987).

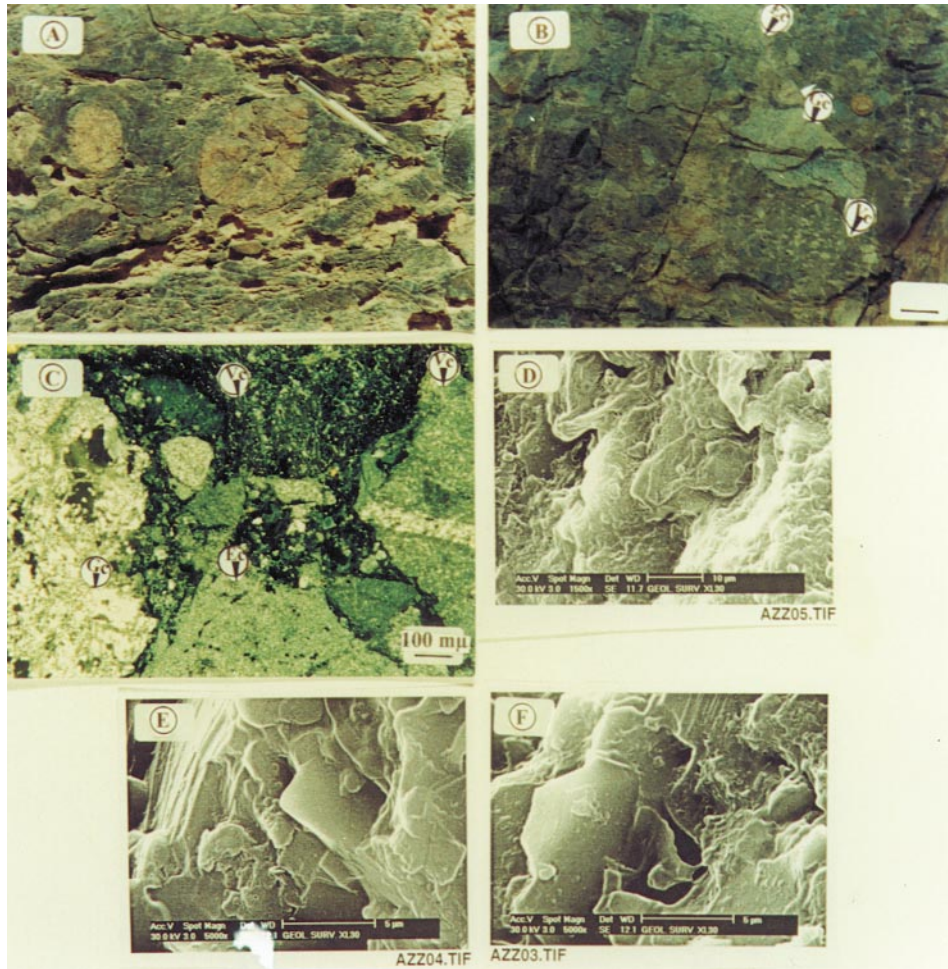


FIG. 7A. Matrix-supported conglomerate encompasses pebbles, mainly of granitic types.
 7B. Crudely stratified clast-supported conglomerate contains mixed clasts of volcanic (V), plutonic (P) and epiclastic rocks (E).
 7C. Photomicrograph shows mixed clasts-supported conglomerates, composed of volcanic (Vc), granitic (Gc) and sandstone (Sc) clasts.
 7D. SEM image shows fine-grained vermicular kaolinite.
 7E. SEM image shows stacked booklets of kaolinite.
 7F. SEM image shows typical kaolinite booklets displaying pseudohexagonal form.

Interpretation: the upper interval is interpreted as a multiple channel conglomerate of mixed origin. The occurrence of such multiple channel in the upper interval suggests turbulent flood waters capable of eroding into the underlying rock sheets (lower and middle interval). The presence of weak horizontal stratification especially in clast-supported conglomerates implies sediment movement as diffuse sheets of sediment (Hein and Walker, 1977) or low-relief longitudinal bars (Smith, 1974). The poor definition of such channel probably reflects the high mobile nature of the sediment load (Stokes and Mather, 2000).

Clay Mineralogy

The nature and distribution of the clay minerals seem to have been controlled by provenance, tectonism, volcanic activity and physical, chemical and diagenic parameters in the basins of deposition. Therefore, clay minerals which result from sedimentation, become an indicator of the nature of those environments (Keller, 1970). Examination of the identified clay minerals by SEM revealed that they have criteria indicative of an authigenic origin such as obvious crystal outlines and undeformed delicate morphologies. Authigenic clay minerals occur widely throughout the studied sandstone and mudstone rocks (Fig. 8).

Kaolinite is the most abundant authigenic clay phase and common in nearly all samples. It has different morphologic characteristics and crystal sizes ranging from microcrystalline booklets to a coarse crystalline variety. It displays well crystallized booklets showing fine-grained vermicular, stacked booklets and pseudo-hexagonal crystal forms (Figs. 7D/E/F). These kaolinite booklets mainly fill the pore space between the detrital grains (see Figs. 5D&6B). Kaolinite requires environmental conditions involving precipitation exceeding evaporation, intense leaching, an excess supply of H^+ ions and removal of ions (Ca^{++} , Mg^{++} , Na^+ and K^+ ions) from the clay-forming system (Keller, 1977). Schwartz and Longstaffe (1988) suggested that over the PH range of 3 to 6, calcite cement continues to dissolve, driving the solution PH to higher values. In contrast, the activity of Al^{3+} drops by several orders of magnitude over the same increase in PH, leading to supersaturation of Al^{3+} and precipitation of kaolinite. Kaolinite in the studied rocks is believed to be formed by the alteration of detrital feldspar as evidenced by: (1) occurrence of kaolinite within the altered feldspar grains (Fig. 5B), (2) an abundance of pore-filling kaolinite near-by the dissolved feldspar grains.

Chlorite is the second less abundant pore-filling authigenic clay mineral in the mudstone rocks. Many of the chlorite stack morphologies have euhedral shapes (Figs. 6G/K), reminiscent of pyroxene/amphibole phenocrysts precursors. Direct precipitation from pore waters during burial is the favored origin of the pore-filling chlorite. The required ions are supplied by mineral

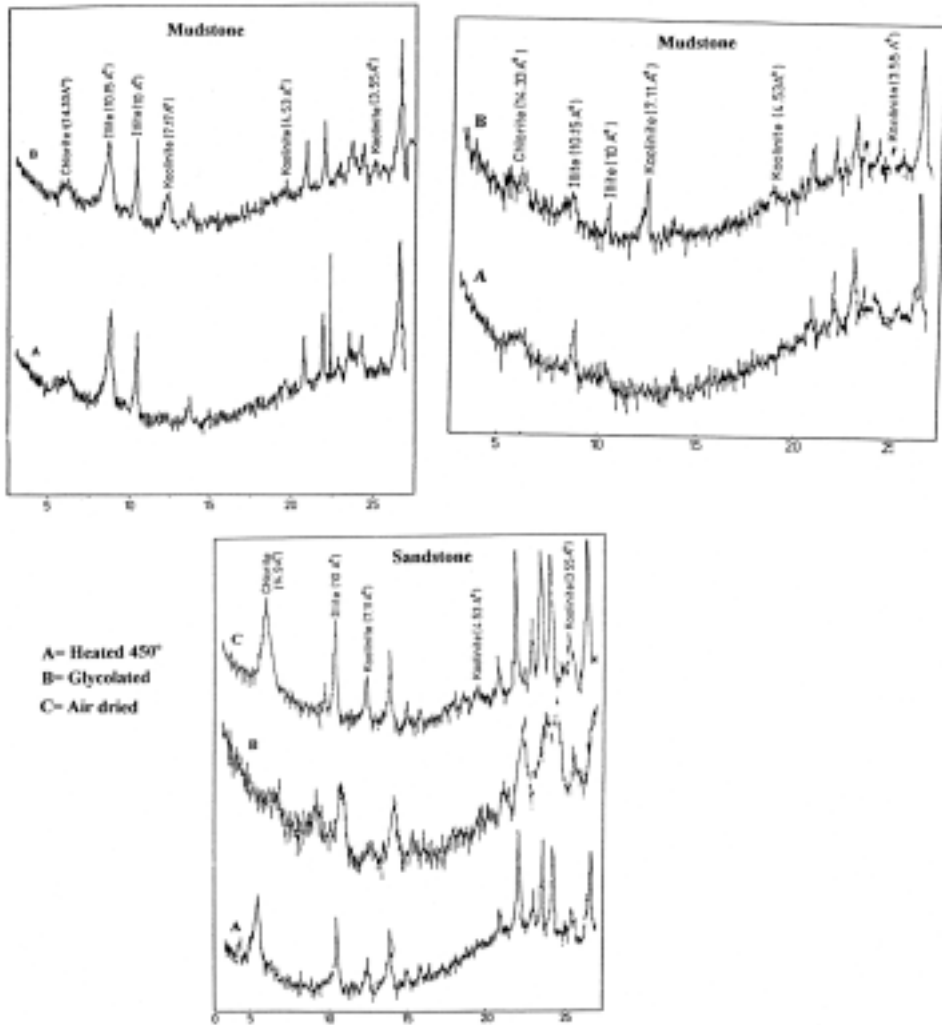


FIG. 8. X-ray diffraction pattern of oriented clay minerals.

decomposition reactions involving detrital silicate minerals (e.g. feldspars). Gradual chemical dissolution of feldspar in these rocks would have released a plentiful supply of Al^{3+} and Si^{4+} solution (Humphreys *et al.*, 1989). Iron and Mg^{++} would have been supplied to pore waters from the breakdown of detrital pyroxene/amphibole. Also, iron may come from river input or meteoric water invasion during subaerial exposure.

Illite is a minor authigenic clay in the studied rocks. XRD analysis helps greatly in the identification of this phase. Illite in some samples shows broad peaks of XRD patterns (Fig. 8) indicating poor crystalline or degraded illite where broad peaks may suggest a diagenetic origin through hydration of mica. Thin sections show presence of filamentous (hairy) textured illite (Fig. 5G) growing into pore space, most probably after mica. It also shows spiny (hairy) illite growing along and in between kaolinite booklets.

Many authors (e.g. Huggett, 1995; Lanson *et al.*, 1996) concluded that illitization can be formed from the alteration of the precursor components (e.g. K-feldspar, kaolinite and mica) in alkaline pore fluid at deep burial (3-4 km) and high temperature (100-120°C). Authigenic illite may be formed through direct precipitation from solution, where the pore solution reaches a relatively high K^+/H^+ ratio by continuous release of K^+ and consumption of H^+ ; under such conditions, kaolinite is not stable. Also, illitization of kaolinite, is suggested as another possible source of illite (Lanson *et al.*, 1996). The breakdown of detrital K-feldspar and mica released the sufficient amount of K^+ required for the kaolinite-illite reaction.

Post Depositional Modifications

The rock units exposed at EL Tarr area consist dominantly of volcanic and associated volcaniclastic sediments. The whole succession has undergone folding and faulting and been metamorphosed to the greenschist facies. Also, evidence for post-depositional modification takes the form of sediment rubification, mottling and carbonate accumulation. Carbonate development is confined to the fine-grained sandstone and mudstone units, occurring as small, randomly orientated nodules up to 2 cm in diameter or within a more organized lattice type framework. Moreover, the diagenesis of the sandstone and mudstone rocks may be summarized as follows: (1) early compaction and fracturing of framework grains; (2) hydration of vitric volcanic rock fragments and to less extent, detrital feldspar grains, with concomitant formation of clay minerals; (3) precipitation of authigenic kaolinite overgrowths on detrital feldspar grains; (4) local precipitation of grain replacive and pore-filling calcite; (5) replacement of detrital mica by illite.

The sediment coloration and carbonate accumulations within the middle stratigraphic interval imply post-depositional modification of primary sedimentary units by pedogenic activity similar to that discussed by Machette (1985) and Retallack (1990). Rubification of the sediments can be attributed to pedogenic reddening or by the reworking of red soils from sediment source areas. Confinement of the rubification to the middle and upper stratigraphic intervals of the conglomerates suggests long periods of subaerial exposure following each depositional event. Such pedogenic modification supports a relatively dry climate with deposition by high magnitude storm events with long recurrence intervals during which pedogenesis occurred (Stokes and Mather, 2000). A lack of well developed pedogenic modification throughout most of the channelized sediments of the middle interval suggests high rates of sedimentation which inhibited soil development. Thick, laminar carbonate developments in the fine-grained sediments of the middle interval are typical of stage IV-V calcrete formation (after Machette, 1985) and probably correspond to a prolonged period of subaerial exposure to arid/semiarid conditions. The term calcrete (Wright and Tucker, 1991) is applied to describe near surface, terrestrial accumulations of predominantly calcium carbonates. It results from cementation, displacive and replacive introduction of calcium carbonate into the soil profile within the vadose zone (pedogenic calcrete). Evidences of pedogenesis are documented by brecciation, mottling and formation of cm-sized carbonate nodules. The main source of calcium carbonate in pedogenic calcrete is wind-blown dust. The Ca-rich dust accumulates in soil surface and is dissolved by rain water (Machette, 1985).

Geochemistry

Nomenclature and Classification of the Volcanic Rocks

The data set (Table 1) has been subdivided into mafic (basalts/andesites) and felsic members. The investigated volcanics exhibit a wide range of composition spanning the entire range from high K-basalt and basaltic andesite through andesite to dacite and rhyolite according to the classification of Peccerillo and Taylor (1976) (Fig. 9A). On the AFM diagram, these volcanic rocks plot in the calc-alkaline field (Fig. 9B). Concerning the paleotectonic setting, the mafic volcanic rocks (basalts/andesites) belong to orogenic volcanics (volcanic arc environment) according to the classification of Pearce (1980) (Fig. 9C).

The mafic rocks (basalts/andesites) range from 50 to 62.30 wt.% SiO₂. They are low in TiO₂ (0.41-0.85), Fe_T (3.99-9.02), MgO (3.80-6.00) and show moderate enrichment in Na₂O, K₂O and P₂O₅. These rocks show also moderate enrichment in large ion lithophile elements (LILE: Sr =130- 893 ppm; Rb = 28-80 ppm; Ba = 373-801 ppm) compared with typical orogenic andesite (Gill, 1981). The felsic rocks contain relatively high concentration of total alkalis

($\text{Na}_2\text{O}+\text{K}_2\text{O}$), LILE (Rb = 74-174 ppm; Ba = 692-731 ppm) and more enrichment in high field strength elements (HFSE: Zr = 255-974 ppm; Y = 27-103 ppm; Nb = 20-77 ppm).

Major/Trace Elements Variations

The whole volcanic rock suite shows progressive decrease in TiO_2 , Fe_T , MgO, CaO and progressive increase in total alkalis, with increasing acidity of this suite (Table 1). It is also characterized by a wide range of trace elements; Sr varies from 112 to 893 ppm, Rb from 28 to 174 ppm, Ba from 409 to 781 ppm, Zr from 99 to 974 ppm, Y from 21 to 103 ppm and Nb from 11 to 76 ppm. There is gradual decrease in Cr (143-0.0 ppm), Ni (116-3.0 ppm) and Co (33-12 ppm) and gradual increase in LILE and HFSE with increasing silica content.

Petrogenesis

The relatively high Cr (102-143 ppm) and Ni (54-116 ppm) for the studied basalts readily allows for generation by partial melting of the upper mantle, followed by limited crystal fractionation of olivine and pyroxene (compare $\text{Mg}^\#$ of 37-47 for basalts with $\text{Mg}^\#$ of > 70 expected for basalt in equilibrium with mantle peridotite; BVSP, 1981). Initial $^{87}\text{Sr}/^{86}\text{Sr}$ for the mafic rocks from the arc-related volcanics in Sinai are = 0.7030 (Halpern and Tristan, 1981) falls well within the range expected for the Late Precambrian upper mantle (Stern and Hedge, 1985). The fact that the Y content in these basaltic rocks is not depleted means that either melting occurred at pressure below the stability field of garnet peridotite (*i.e.*, shallower than about 60-75 km; Danckwerth and Newton, 1978), or that garnet was consumed. Concentration of Cr (av. ~ 119 ppm) and Ni (av. ~ 78 ppm) for the studied basalts would be much lower if removal of large amounts of pyroxene and olivine has occurred. All the basaltic samples have low Sr content (up to 250 ppm), indicating that either plagioclase remained in the mantle after melting, or was fractionated from the evolving melt; the petrographic observations showed that the melts were saturated in plagioclase leads to prefer the latter interpretation. Considering that olivine, pyroxene and plagioclase were likely near-liquidus minerals and that relatively minor separation of the first two could have occurred; it is suggested that separation of less than perhaps 30% solids from primary mantle melts resulted in the basaltic rocks analyzed in Table (1).

Fractional Crystallization Model

Increasing incompatible element concentrations (LILE & HFSE) and decreasing compatible element concentrations (V, Cr, Ni, Co) with increasing silica content throughout the investigated lava are consistent with a model

TABLE 1. Chemical compositions of the volcanic and sedimentary rocks at Tarr area, SE Sinai, Egypt.

No.	T.5	T.9	K.7	K.8	K.2	K.3	K.4	K.5	T.2	T.3	T.4	K.13	R.1	R.2	R.3	R.4	R.5	R.6
Type	B	B	B	A	A	D	R	R	SS	SS	SS	SS	SS	SS	SS	SS	SS	SS
SiO ₂	50.42	52.90	51.9	62.3	59.2	65.9	69.92	71.16	59.80	50.5	51.6	53.57	58.19	61.83	55.79	71.66	76.79	83.79
TiO ₂	0.41	0.79	0.59	0.85	0.75	0.30	0.35	0.34	0.61	0.7	0.36	0.64	1.77	1.57	0.81	0.63	0.44	0.49
Al ₂ O ₃	5.15	15.30	14.30	14.5	15.9	13.8	14.58	14.25	16.20	16.4	15.2	14.49	15.77	14.93	15.37	11.80	10.82	7.36
Fe ₂ O ₃	9.02	5.74	7.85	3.99	6.39	4.94	1.99	1.85	4.80	4.85	11.85	6.00	7.68	6.28	6.28	3.84	2.58	2.12
MgO	5.19	5.00	6.00	3.80	2.40	1.20	0.74	0.65	2.60	5.00	3.60	2.86	3.53	1.87	2.57	1.43	0.90	0.98
CaO	10.17	11.20	9.80	4.36	4.48	2.24	1.57	1.42	5.36	4.92	6.16	3.62	5.04	3.43	6.65	2.54	1.16	0.18
Na ₂ O	5.05	4.73	4.59	5.85	6.75	5.24	5.43	4.51	5.21	5.72	6.95	4.13	5.12	4.25	4.49	2.43	2.27	1.36
K ₂ O	2.11	1.67	1.48	2.17	1.94	3.55	3.47	3.85	2.10	2.17	1.29	2.59	3.00	3.40	1.10	1.73	2.65	1.30
P ₂ O ₅	0.36	0.31	0.33	0.34	0.32	0.31	0.11	0.10	0.32	0.34	0.32	0.30	0.24	0.56	0.18	0.12	0.08	0.13
L.O.I.	2.13	1.65	2.16	1.20	0.95	1.25	0.78	0.86	2.10	7.75	2.45	1.80	0.16	0.13	6.07	3.42	2.23	2.12
Total	100.0	99.29	99.00	99.4	99.00	98.7	98.94	99.04	99.10	98.4	99.78	100.00	99.90	93.34	99.53	99.68	99.97	99.85
Co	26	33	10	22	23	12	10	13	7	6	31	7	-	-	18	12	10	5
V	123	156	139	394	469	145	20	29	28	24	156	30	-	-	131	89	48	31
Cr	102	143	111	62	33	25	0.00	0.00	52	38	154	52	-	-	37	51	26	39
Ni	54	65	116	15	8	3	0.00	0.00	12	12	65	8	-	-	11	13	10	8
Cu	28	44	46	<2	<2	<2	0.00	0.00	7	8	40	8	-	-	23	11	8	6
Zn	136	77	60	116	107	78	22	41	69	125	76	41	-	-	89	74	52	26
Ga	14	17	21	20	22	22	0.00	0.00	15	11	20	14	-	-	17	13	14	16
Pb	6	17	29	5	6	6	0.00	0.00	24	22	18	24	-	-	6.9	15	24	66
Rb	66	28	44	75	80	174	62	74	33	35	13	9	-	-	18	67	115	61

TABLE I. Continued.

No.	T.5	T.9	K.7	K.8	K.2	K.3	K.4	K.5	T.2	T.3	T.4	K.13	R.1	R.2	R.3	R.4	R.5	R.6
Type	B	B	B	A	A	D	R	R	SS	SS	SS	SS	SS	SS	SS	SS	SS	SS
Sr	250	130	112	893	881	321	308	287	196	322	136	330	-	-	637	250	141	66
Ba	409	373	801	783	629	731	516	692	135	130	343	106	-	-	370	444	522	253
Zr	147	146	99	298	273	974	255	270	200	155	167	177	-	-	96	229	179	298
Y	21	21	22	63	41	103	45	27	64	50	24	57	-	-	19.5	24	24.9	27.3
Nb	27	29	11	76	33	77	50	30	22	22	31	25	-	-	2.00	8.5	10.7	7.9
Mg#	37	47	43	49	29	20	25	27	38	53	25	35	-	-	-	-	-	-
K/Rb	265	495	279	240	201	169	464	431	528	514	823	2591	-	-	578	219	189	178
Zr/Y	7.00	6.95	4.50	4.73	6.66	9.46	5.67	10	3.13	3.10	6.96	3.11	-	-	5.67	9.6	7.2	12.4
Nb/Y	1.29	1.38	0.5	1.21	0.80	0.75	1.11	1.11	0.34	0.44	1.29	0.44	-	-	0.11	0.36	0.43	0.30
Rb/Y	3.14	1.33	2.00	1.19	1.19	1.68	1.38	2.74	0.52	0.70	0.54	0.16	-	-	0.92	2.79	4.62	2.23
K/Na	0.42	0.35	0.32	0.37	0.92	0.68	0.64	0.85	0.40	0.38	0.19	0.63	0.59	0.80	0.24	0.71	1.17	1.00
Al/Si	0.30	0.29	0.28	0.23	0.27	0.21	0.21	0.20	0.27	0.32	0.290	0.23	0.27	0.24	0.28	0.16	0.14	0.09
Fe+Mg	14.21	10.7	13.85	7.79	8.79	6.14	2.73	2.50	7.40	9.85	15.45	8.86	11.21	8.15	8.85	5.27	3.48	3.10

Code:

Fe₂O₃: total iron as Fe₂O₃.

L.O.I.: wt% loss on ignition.

Mg# : {MgO/Fe₂O₃ + MgO} × 100.

R1 & R2: chemical composition of sandstone rocks, wadi Kid area (EL-Gaby *et al.*, 1991).

R3, R4, R5 & R6: Major and trace elements characteristics of greywackes from various tectonic settings (Bhattia and Crook, 1986).

R3: oceanic island arc; R4: continental island arc; R5: active continental margin; R6: passive margin

B = basalt; A = andesite; D = dacite; R = rhyolite; SS = sandstone.

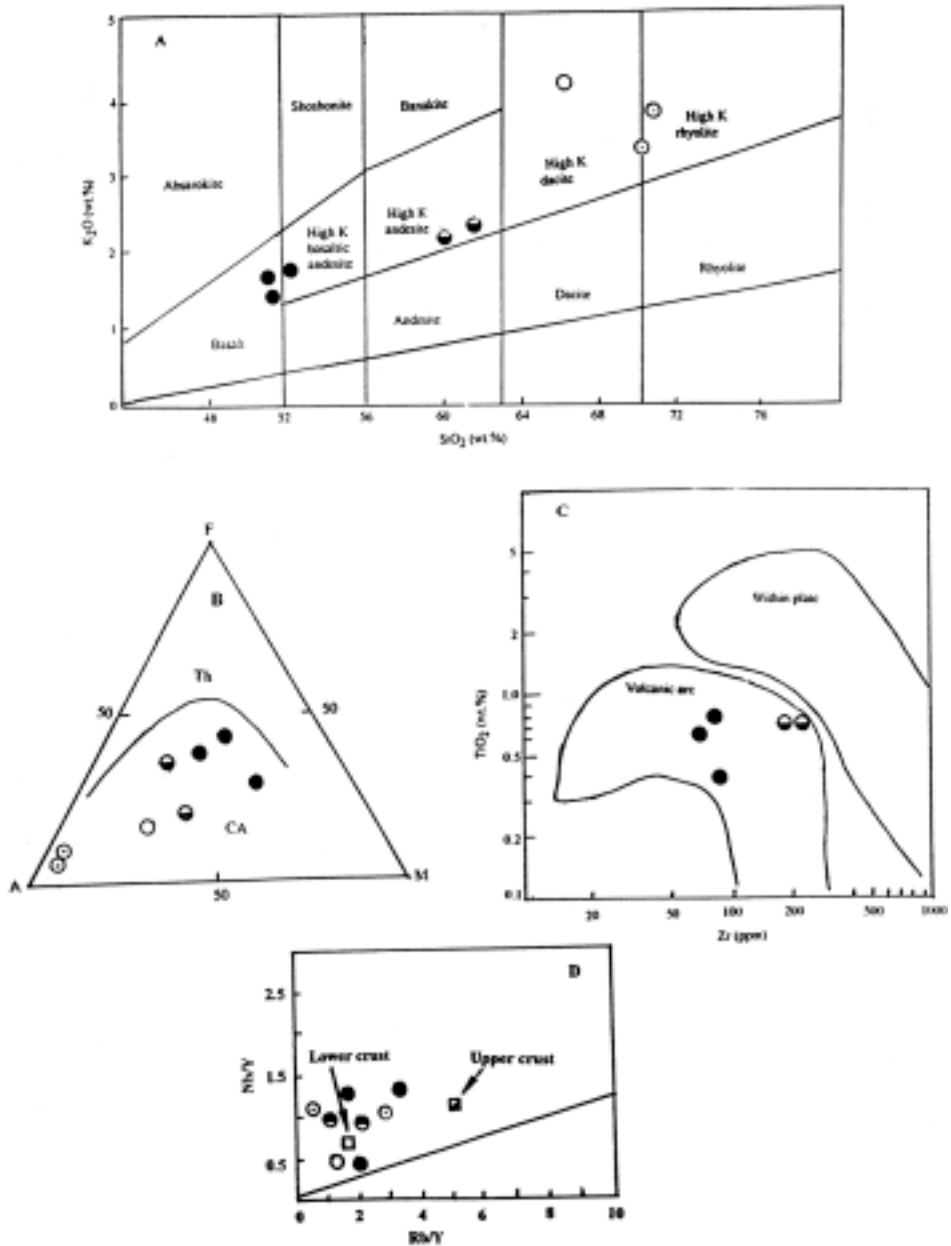


FIG. 9. Geochemical characteristics and the inferred tectonic setting of the studied volcanic rocks. (A) SiO₂ versus K₂O classification binary diagram (Peccerillo and Taylor, 1976); (B) AFM ternary diagram (Irvine and Baragar, 1971); (C) Zr versus TiO₂ binary diagram (Pearce, 1980); (D) Nb/Y versus Rb/Y diagram (Chazot and Bertrand, 1995): The upper and lower crust compositions are from Taylor and McLennan (1981) and Weaver & Tarney, (1981) respectively.

involving the crystal fractionation of the plagioclase + pyroxene + hornblende + opaque + apatite, from a parent basaltic magma. Similarly, the constancy of the ratios of all high incompatible trace elements Rb, Nb, Y (Table 1) from basalt to rhyolite, is a feature diagnostic of co-magmatic volcanic series generated by crystal fractionation process (Treuil and Varet, 1973).

Separation of an assemblage of pyroxene, plagioclase, opaque and apatite, the dominant phases within the basalt to andesite interval, is consistent with the observed increase in SiO_2 , K_2O , Na_2O and incompatible element contents, and the decrease in Al_2O_3 , MgO , CaO , Co, Cr, Ni and V content with fractionation. The andesite to dacite/rhyolite interval reflects a pronounced change in the nature of the separating phase assemblage. Rapid decreasing Sr in siliceous liquids suggests that plagioclase may become more modally important within the solid removed during this stage. These observations support a separating phase assemblage dominated by plagioclase, hornblende, opaque and apatite. The results of the least squares mass balance calculations (not shown in this study) indicate that andesite may be generated by 59% crystallization of the parent basalt on the removal of a solid assemblage dominated by Cpx (25%), plag (54%), Op (11%) and Ap (10%). Dacite/rhyolite may be generated by ~20% of an intermediary andesite. The solid removed is again dominated by Hb (23%), plag (55%), Op (13%) and Ap (9.0%).

The useful index to differentiate between crystal fractionation and crustal contamination is given in Fig. (9D) using trace element ratios such as Nb/Y versus Rb/Y (Chazot and Bertrand, 1995). In Nb/Y versus Rb/Y diagram, all of the investigated rock samples plot relatively close to lower and upper crustal values (Taylor and McLennan, 1981; Weaver and Tarney, 1984) respectively. Hence, crustal contamination may be superimposed on crystal fractionation in the evolution of Kid volcanics.

Many lines of evidences indicate the existence of high level magma reservoir (*i.e.* shallow magma chamber) within the crust beneath the Kid area. These evidences include petrological evidences for the role of low pressure crystal fractionation involving Cpx, Hb, plag, Op and Ap and the existence of intrusive plutonic suites (Wilson, 1989). In general, such shallow crustal chamber (less than 20 km) is associated with ancient andesites and basalts or basaltic andesites which evolved in magma chamber situated at the mantle (40 to 100 km, Gill, 1981).

Geochemical Characteristics of Volcanogenic Sandstones

The chemical composition of sedimentary rocks records the nature and proportions of their detrital components from which their provenance may be postulated. These rocks may even undergo metamorphism to greenschist-amphibolite facies, but still retain their provenance signatures (Roser and Korsch, 1988).

The sandstone of this study has an SiO_2 range of 50.5-63.57 wt.%, high to moderate $\text{Fe}_2\text{O}_3\text{T} + \text{MgO}$ values of 7.4-15.45% and $\text{Al}_2\text{O}_3/\text{SiO}_2$ ratios that range from 0.23 to 0.32 with most around 0.28. TiO_2 contents are less variable, ranging from 0.36 to 0.7%, while the ratio of $\text{K}_2\text{O}/\text{Na}_2\text{O}$ is less than unity (Table1). These rocks are characterized by a wide range of some trace elements: V = 156-24 ppm; Cr = 154-33 ppm; Ni = 65-8.0 ppm; Rb = 35-9 ppm; Sr = 330-136 ppm; Ba = 343-106 ppm. HFSE does not show much variations (Zr = 200-155 ppm; Y = 64-24 ppm; Nb = 31-22 ppm).

Using bulk chemistry, Roser and Ktorsch (1988) plotted Harker variation diagrams of parameters that they thought were most discriminating to infer four primary provenance groups namely P_1 , P_2 , P_3 and P_4 (Fig. 10). All the rock data mostly fall in both P_1 and P_2 to varying degrees, indicating a provenance of mafic and intermediate igneous provenances. But in $\text{K}_2\text{O}/\text{Na}_2\text{O}$ and $\text{Al}_2\text{O}_3/\text{SiO}_2$ versus $\text{FeT} + \text{MgO}\%$ diagrams, rock data plot in three former groups ($P_1/P_2/P_3$) and support the suggestion that a volcanic/plutonic-rich continental provenance was dominant. This conclusion is supported by the petrographic investigations. The presence of lathwork and vitric textures, reflect derivation from basaltic rocks. Moreover, microlitic or felsitic textures are of intermediate to felsic volcanics. These sandstone rocks contain small but significant biotite and oscillatory-zoned plagioclase, suggesting derivation from arc andesite. Volcanic and pyroclastic interbeds with epiclastic sandstone also attests to contemporaneous explosive volcanism. This empirical test suggests that the composition of arc-derived epiclastic sandstone may record periods of explosive arc magmatism with little or no time lag.

Concerning the tectonic setting determinations, the studied sandstone rocks show great discrepancies in both major/trace element compositions if compared to those elements in greywackes from island arc and passive margin environment (Fig. 11). The sandstones, dominantly derived from volcanic rocks, resemble the active continental margin in major and trace elements except high Na_2O , Nb and Y characterizing the investigated sandstone rocks. The compositional immaturity of sandstone, is probably due to high sedimentation rates, characteristic of tectonically active regions, coupled with the general absence of mineralogically stable detritus supplied by the volcanic arc and reworked older units (Lundberg, 1991).

Discussion

Sedimentation patterns in modern and ancient examples of marginal basins are complex. Resedimentation of large volumes of remnant and syn-extensional volcanic products occurs in a variety of settings (Lonsdale, 1975). Compositional analysis of epiclastic deposits in recently active island arc, active con-

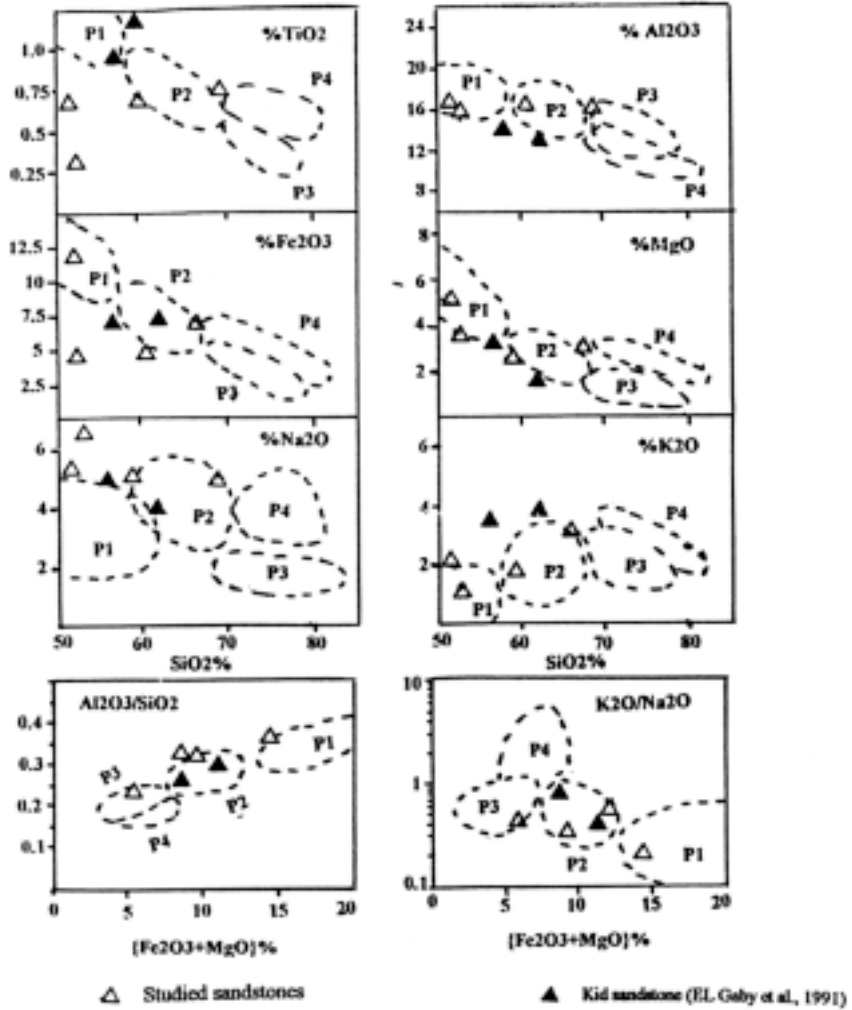


Fig. 10. Harker variation diagrams of major elements plotted against SiO_2 and $\text{K}_2\text{O}/\text{Na}_2\text{O}$ & $\text{Al}_2\text{O}_3/\text{SiO}_2$ ratios versus $\{\text{Fe}_2\text{O}_3 + \text{MgO}\}\%$ for sandstone. The broad fields of Roser and Korsch (1988) are outlined: P_1 = mafic igneous provenance; P_2 = intermediate igneous provenance; P_3 = felsic igneous provenance and P_4 = quartzose sedimentary provenance.

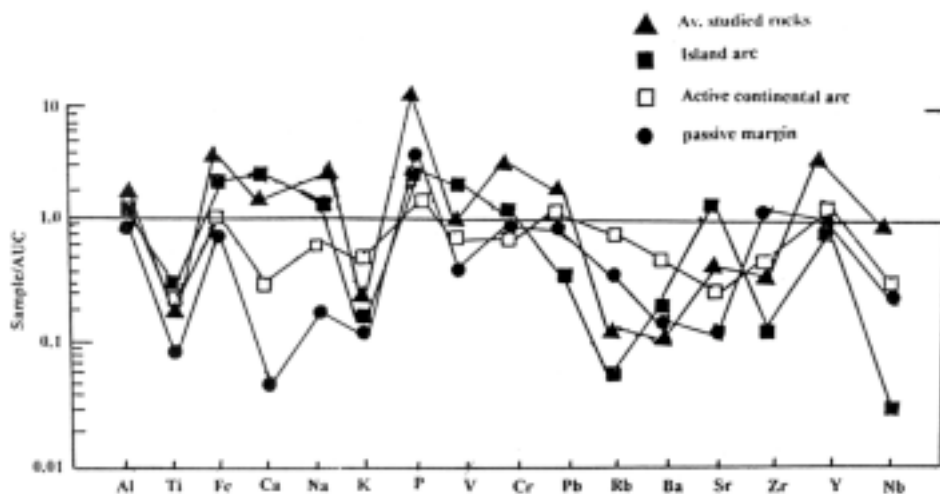


FIG. 11. Spider diagram shows comparison of the studied sandstone with sandstone from various tectonic settings. The normalization value of average upper continental crust (AUC) is taken from Taylor and McLennan (1981).

tinental margin and back arc basins (Dickinson and Valloni, 1980) has revealed that sediment distribution is governed by a variable interplay of sediment source (provenance), tectonic and climatic factors.

Sediment Source

The structural arrangement and variable lithology of the basement of the Kid area allows for the main sediment source areas of the El Tarr basin to be established. Provenance has been established through the analysis of clast assemblages derived from sandstone and conglomeratic units within the alluvial fan and braided river components. Clast provenance within the study area typically comprises the Kid volcanics. These volcanics encompass subaerial volcanic lava flows and pyroclastic deposits of calc-alkaline, high-K basalt, andesite, dacite and rhyolite as well as hypabyssal felsic intrusive rocks. The predominance of calc-alkaline composition, the great abundance of andesitic to rhyolitic rock associations and their plotting in the orogenic environment favour an active continental margin tectonic setting of Kid volcanics. The most striking feature of these rocks is their high concentration of large ion lithophile elements (Sr, K, Rb, Ba) and depletion in Ti, Zr and Cr characteristic of calc-alkaline lavas. All these features are characteristic of lava erupted in anomalous volcanic arc setting (Pearce, 1982). The anomalous volcanic arc lavas are explained by Pearce (*opt. cit.*) as either derived from mantle sources that suffered at least two episodes of enrichment, one related to the subduction and the other unrelated, or by mixing of magmas from two distinct sources. The predominant intermediate

to felsic composition and the high Zr/Y ratio (from 4.5 to 9.46) favour a continental arc setting and suggest involvement of subcontinental lithosphere in magma genesis of Kid volcanics. Clasts from the braided river sediments also recorded two key clast assemblages. This suggests that the dominant sediment source area for the braided river sediments was derived from a zone of mixed clast assemblage composition, where sediment was derived from both volcanics and plutonic rocks of variable lithology in a region of fan coalescence. Hence, the Kid volcanics and their felsic derivative rocks which form the surrounding mountain ranges and underlie the basin of the study area comprise a series of lithologically and stratigraphically distinct units which are important in terms of provenance for El Tarr volcaniclastic sediments examined by this study.

These volcanics bear the characteristic lithological and geochemical features of the Dokhan volcanics, at the type locality Gabal Dokhan, northeastern Desert, Egypt. Moreover, the chemical composition of the analysed volcanics and their acidic differentiates are highly comparable with those of cordilleran or Andean-type continental margin orogenic belts, a tectonic setting envisaged by EL-Gaby *et al.*, (1988) for the Dokhan volcanics. The same conclusion was reached by many authors (e.g. Furnes *et al.*, 1985; EL-Gaby *et al.*, 1991) for the Dokhan volcanics at Kid area.

Tectonic Control

Facies analysis provides the evidence for faulting during volcanic and volcaniclastic development. Substantial contemporary tectonic activity is indicated by the switches from proximal fluvial incision through alluvial or overbank deposits, to the proximal braided sediments (lower through middle to upper stratigraphic intervals), repetitive cycles of grain size and bed thickness variations and apparently abrupt up-ward progradations of catastrophic avalanching of very coarse debris (upper interval). Coarsening-upward sequence is common in alluvial fan deposits. So, the combination of features indicative of relatively abrupt sedimentary changes is interpreted as recording active faulting. The sedimentary responses are similar to those of the most actively subsiding strike-slip (pull-apart) sedimentary basins, whose time-averaged subsidence rates are 2-3 km/m.y. (Nilsen and Sylvester, 1995). In some recent studies, large strike-slip zones are regarded as being the important tectonic features in the Arabo-Nubian shield; they are associated with extensional structures such as sedimentary basins and dyke swarms (Stern, 1985). Direct field evidence for deformation of alluvial fan sediments of EL Tarr area can be observed in the cliff section at the entrance of wadi EL Tarr. This locality covering approximately 0.5 km², within which alluvial fan sediments have been tilted and faulted. Volcaniclastic sediments (middle interval) have become tilted, with beds dipping consistently at 20°

NE (Fig. 5C). The fault plane strikes NNW-SSE and is typically steep (60° - 80°). Slickenfabric demonstrates that faulting is of a normal, extensional type. Outside this zone, the planar shear fabric foliation that is widespread in the volcanics, gradually intensifies to mylonitic or phyllonitic foliation along the trace of the thrust. The main units of the Kid, Malhak, Heib and Tarr Fms. are juxtaposed along broad ductile shear zones, interpreted as thrust faults and are linked to a conjugate set of NW and NE-trending megashear (Shimron, 1980). Structurally, the orogenic history in Kid area started with a period of compression and crustal thickening (D1). In this period, compression caused by subduction was responsible for D1 deformation phase. Volcanics of the Heib and Tarr Fms were deposited prior to 620 Ma. NE-SW directed compression related to Precambrian accretion tectonics resulted in the formation of NW-SE trending, high to medium temperature ductile thrusts inherited within wadi Kid (Sakran, 2000). These ductile thrusts were reactivated later by left lateral transgression which may be related to the Najd fault system. During the Najd system (extensional phase), sedimentation, dyke swarms and granitic rocks were formed (Blasband *et al.*, 1997). Moreover, fault cliffs/scarps (Fig. 5C) are common features in Precambrian rocks that resulted from active strike-slip faulting (Sakran, 2000).

This case study clearly demonstrates that tectonics have played an important role during the evolution of the El Tarr alluvial system. Tectonics have (1) provided the gross topography to facilitate fan development, (2) affected sediment supply to the alluvial system by controlling the topographic configurations of the catchment and thus influencing sediment transfer processes to the alluvial system, (3) influenced local geomorphic gradients leading to changes in unit stream power and thus erosive capability of geomorphic processes, (4) generated significant changes in both local and regional base-level.

(1) Gross topographic configuration

Long-term records of alluvial fan sedimentation are most prolific in fault-controlled piedmont settings where tectonics has provided the essential topographic configuration, *i.e.* an uplifted hinterland and an adjacent, subsided sedimentary basin (Stokes and Mather, 2000). Regional tectonics within south Sinai has created a basin and range topography.

(2) Sediment supply to the alluvial system

It is well documented that the topographic configuration of fan catchment areas is a significant control on the processes of sediment transfer to the alluvial fan (Kostachuk *et al.*, 1986; Harvey, 1997). Small, steep catchment areas are typically associated with debris flow processes. Larger and less rugged catchments tend to be associated with more fluvial types of process. This in part re-

flects the steepness of slopes required to generate sediment gravity flows (*i.e.* debris flows) and the water:sediment ratio reaching the fan feeder channel. The presence of debris flow deposits within the lower and upper stratigraphic interval suggests that small, steep catchment areas were supplying sediment to the alluvial fan and braided rivers. Fluvial processes (middle interval) only appear to become dominant after significant catchment area expansion.

(3) Local geomorphic gradients

Tilting of a geomorphic surface may have one of two effects on an alluvial system: (i) where the deformation is perpendicular to stream flow, tilting will result in an increase in unit stream power leading to incision., (ii) where the deformation is more oblique to stream flow, deflection of the stream may occur into the area of maximum subsidence (Alexander and Leeder, 1987). In the case of the deformation observed in the study area both effects can be demonstrated. Relative uplift of the Kid volcanics in the northern part stimulated an increase in local gradients in El Tarr area in the southern part. This stimulated a progressive headward incision which propagated up fan from the point of deformation. This initial incision is marked by the development of solitary channels (lower and middle stratigraphic intervals). During the later stages of evolution, the developing braided river system occupied the topographic low generated by the deformation. This resulted in braided river sediments (upper stratigraphic interval) being deposited over the proximal and distal alluvial fan volcanic environment (lower and middle stratigraphic intervals).

(4) Local and regional base-level changes

Alluvial fans, which are typically dominated by debris flow and sheetflood processes, are insensitive to regional base-level changes until they become fully entrenched (Harvey *et al.*, 1999). Regional base-level changes controlled incision and catchment area expansion. This had profound implications for the volumes of sediment and water feeding the alluvial system. Resulting increases in sediment and water discharge are recorded by the braided river deposits of the upper stratigraphic interval. Continued incision by the river system reflects the basin-wide incision and drainage net expansion. This incision was driven by a combination of regional tectonics and climate (Harvey, 1987).

Climatic Control

Evidence for regional climatic conditions during the Late Proterozoic time is sparse due to the continental nature of the sedimentary basin fills in Kid area. Sedimentary, red colouration and calcareous paleosoil evidence from the alluvial fan deposits, supports a climate characterized by infrequent, high magnitude

storm events typical of dry conditions. Indeed, several studies of ancient and modern fans in SE Spain, have proposed that climatic change was a possible controlling factor for sediment supply and incision into fan surfaces (Stokes and Mather, 2000).

The volcanic complex and associated volcanoclastic sediments are assigned to the arc-flank province because they share several important lithostratigraphic characteristics and suggest a common paleogeographic setting. Most important is that all arc-flank complexes contain 30% to 70% epiclastic sandstone, conglomerate, and mud/siltstone, all or almost all of which accumulated in non-marine environment in which pronounced topographic relief episodically developed (Dunne *et al.*, 1998). Development of such relief is indicated by the abundance of conglomerates, much of which is interpreted to have been deposited by debris flows and debris floods on alluvial fan (Ritter *et al.*, 1995). Rock units in arc-flank volcanic complexes are interpreted to have accumulated principally on river flood plains and alluvial fans and local eolian dune fields. The volcanic strata in arc-flank complexes consist of subequal amounts of lava and pyroclastic deposits. Most lava is andesitic to felsic rocks, possibly reflecting true continental crust (Greene *et al.*, 1997). Volcanic vent was probably located within a few kilometers of some present exposures of arc-flank complex, based on the presence of locally abundant hypabyssal intrusions, some of which are lithologically similar to nearby volcanic units, and on the presence of rhyolite lava flows in the Kid area.

Both uplift of a source area and subsidence of the basin floor seem likely to have been involved in maintaining or episodically re-establishing the nonmarine depositional setting of the arc-flank province. Uplifted source areas in the arc-core province could have been created by any combination of the following processes: (1) construction of large, high standing volcanic edifices, perhaps supplemented episodically by significant magmatic inflation; (2) isostatic response to heating and thickening of the arc-core region by widespread magmatism; and (3) isostatic response to crustal thickening caused by contractional deformation (Bjerrum and Dorsey, 1995). Subsidence of the basement of the arc-flank province almost certainly facilitated accumulation of volcanic and epiclastic strata. Subsidence within arc may have multiple origins (Ingersoll and Busby, 1995), but isostatic response to surface sediment loading is likely to have been a principal contributor, given that the province was subjected to ongoing influx of sediment from higher source areas.

Depositional Environment of the Volcanoclastic Rocks

High-energy alluvial systems (*e.g.* alluvial fans and braided rivers) are commonly observed features within ancient and modern mountain front settings where they typically provide a linkage between a tectonically controlled upland

drainage basin and a lowland sedimentary basin. The complexities of the controls on alluvial environments are well documented (Ritter *et al.*, 1995; Harvey, 1997). These controls operate over a variety of spatial and temporal scales but it is tectonics that govern the overall positioning and long term evolution of alluvial systems. Tectonic activity, particularly through source area uplift and/or direct deformation along fault controlled mountain front settings, can affect alluvial system by (1) determining the spatial location of alluvial fans/streams, (2) uplift and tilting of geomorphic surfaces, and (3) controlling the positioning of local and regional base-levels. The resultant sedimentary response to these controls is complex, but is typically characterized by deflection of alluvial systems away from the area of maximum uplift or changes in the aggradational/dissectional behaviour of the alluvial system.

The volcaniclastic sediments in the study area have a volcanic/plutonic provenance and lack the features considered diagnostic of base-surge deposition (*e.g.* massive accretionary lapilli-rich interbeds). The predominance and nature of the sedimentary structures present (*e.g.* wavy-planar to low-angle cross lamination) are suggestive of tractional fluvial deposition (Bull, 1993). The preservation of these types of sedimentary structures is widely considered to represent deposition during flood events in ephemeral streams (*e.g.* McKee *et al.*, 1967; Tunbridge, 1981), because, in perennial systems, flood deposits are reworked during periods of normal current activity, resulting in abundant cross-bedded deposits. The presence of massive sandstone rocks which grade both laterally and vertically into the stratified fine/medium-grained sandstone and mudstone (middle interval) is also consistent with an ephemeral stream interpretation (Bull and Cas, 2000). Such massive deposits are common in these systems, where they are interpreted to represent deposition from turbulent, high-sediment concentration (*i.e.* hyperconcentrated; Smith, 1986) flows during periods of high discharge.

The presence of debris flow and sheet flood deposits which have been subjected to pedogenesis imply an alluvial fan environment (Bull, 1972; Blair and McPherson, 1994). The spatial arrangement of debris flow deposits dominating in proximal areas and sheet flood dominating in distal areas is also considered to be characteristic of alluvial fans (Harvey, 1997). Authors like Glass (1958) and Pryor and Glass (1961) have generally considered kaolinite which is the predominant authigenic clay in the studied rocks, to be dominant in fluvial environments. It is plausible now to suggest that the abundant kaolinite, present in sandstone/mudstone, was formed under a continental and/or non-marine environment "fluvial conditions". The fact that kaolinite is very well crystallized supports its formation in a continental environment and is in accord with the view of Keller (1970). An alluvial fan environment is further supported by the

preservation of several paleolake beds at different elevations in wadi Feiran system, in the northwest of the study area (Awad, 1953). Most of the paleolakes in Sinai Peninsula were probably ephemeral features (Issar and Eckstein, 1969).

Later, these studied volcanoclastic sediments bear the characteristic lithological features of the Hammamat sediments, at the type locality of wadi EL-Hammamat, central Eastern Desert, Egypt. The intercalations between the volcanics and sediments, poorly-sorting of these sediments and the preservation of the volcanic fabric in the clasts within these volcanoclastic sediments indicate that the Dokhan volcanics and the Hammamat sediments are penecontemporaneous and a narrow time span between eruption and sedimentation, as suggested by El-Gaby *et al.*, (1988). Generally, the Dokhan volcanics differ from the "Shadli" metavolcanics in their high potash content, abundance of felsic differentiates and common presence of ignimbrites and welded tuffs. The Hammamat sediments differ from the island arc metasediments by the presence of clay minerals, high potash and aluminum contents and absence of intercalation banded iron formation (EL-Gaby *et al.*, 1991).

Tectonostratigraphic Model

In order to account for the observed paleogeographic changes, a model is proposed which incorporates the sedimentary, stratigraphical and tectonic evidence recorded within the study area (Fig. 12).

(i) Early stage: alluvial fan progradation

The early stage of the EL Tarr succession reflects the development of proper proximal alluvial fan bodies. Low-frequency, high-magnitude storm events during a dry climate supplied sediment to the fan bodies through debris flow and sheet flood processes, sourced from the NW part of the study area (Kid volcanics). This initial progradation is reflected stratigraphically, by an overall, local-scale fining upwards succession (lower stratigraphic interval). Fining-upward sequences on a scale of tens of metres suggest switching of active fan area sedimentation during progradation.

(ii) Mid-stage: localized deformation and fan abandonment

Continued aggradation of fan sediments (distal facies) is characterized by the stacking of sequence scale (metres to tens of metres) fining-upwards successions. This stage suggests switching of the active fan area sedimentation during progradation to inactive flood plain (middle stratigraphic interval). The transition from lower to middle interval is depicted by a phase of extensional deformation, which generated differential uplift and subsidence between the northwest and

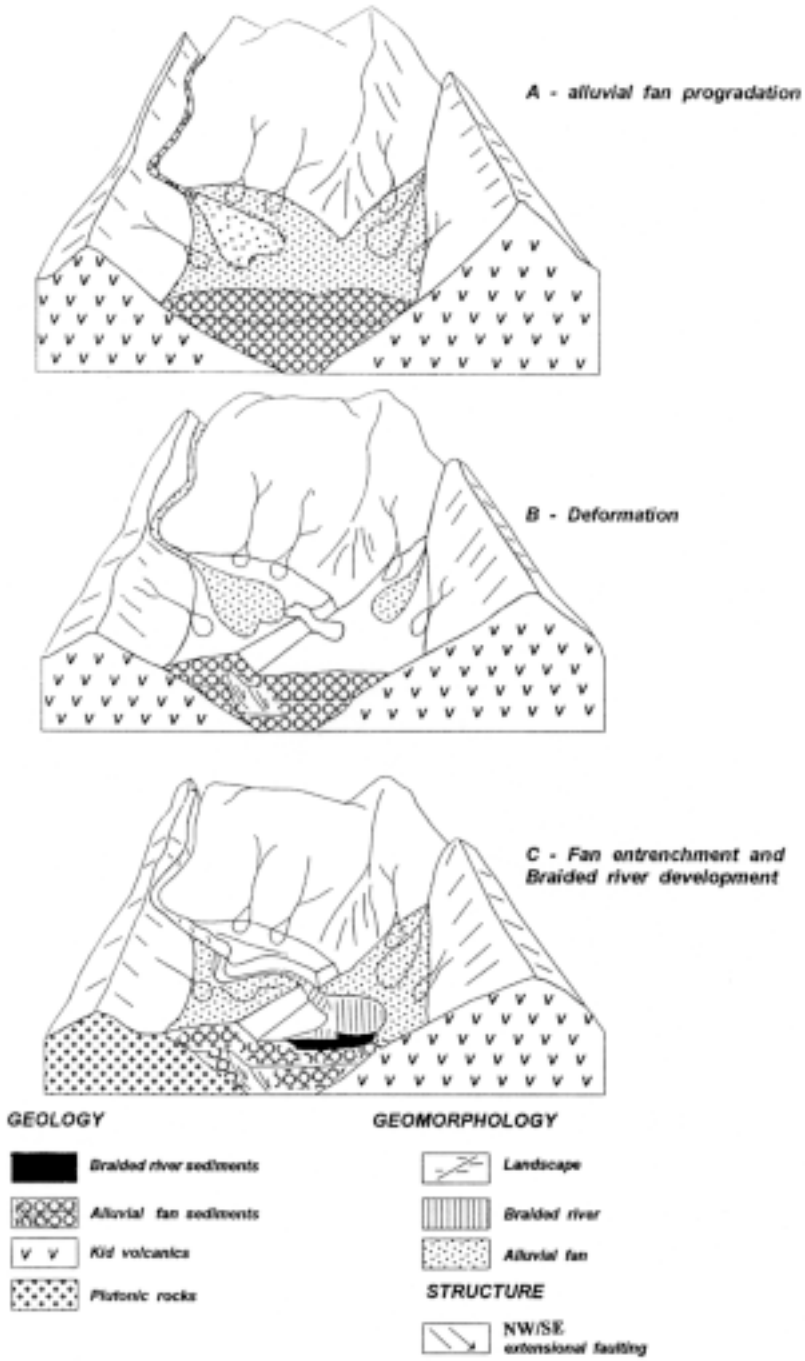


Fig. 12. Proposed depositional and structural evolution of the volcaniclastic sediments in the El Tarr area, southeastern Sinai, Egypt.

southern alluvial fan. Relative subsidence of the southern part (Tarr area) and uplift of the northwestern part (Kid volcanics) stimulated incision into the northern part. Sediments liberated by this incision were transported basinwards by isolated solitary channels.

(iii) Late stage: fan entrenchment and braided river development

The final stage has a distinct change in depositional style and sediment routing. The lower and middle interval became abandoned and upper interval, sourced entirely from Kid volcanics and plutonic rocks was established. It is characterized by continued uplift, and expansion of the catchment area in EL Tarr area, feeding the newly formed braided river system. Uplift would lead to catchment area expansion through headward erosion of tributary streams and through river capture events. The resultant enlargement in catchment area would increase the magnitude of runoff generation and sediment load during flood events, and thus could account for a switch to a more fluvial type of deposition, in this case by the occurrence of ill-defined, highly mobile, multiple channels for a braided river system. The multiple channel system was bedload-dominated and characterized by bedload movement in the form of diffuse gravel sheets and longitudinal bars in highly mobile channels. This is typical of sedimentation in braided river systems as described by Williams and Rust (1969), Smith (1974), Hein and Walker (1977) and Miall (1978). The increase in maximum clast size and percentage of conglomerates towards the top of the upper stratigraphic interval would appear to indicate an increase in sediment discharge and caliber associated with a multiple channel, proximal braided river system (Stokes and Mather, 2000). Similar effects have been recorded in alluvial river systems where changes in river platform and long profile in response to active tectonics have been documented (Ouchi, 1985). Where tectonic activity is of sufficient magnitude and frequency, river systems have also been shown to have been deflected away from the area of maximum uplift (Alexander and Leeder, 1987). Within the sedimentary record these effects are revealed by changes in alluvial architecture, provenance and sedimentary style. Indeed, the relative lack of well developed pedogenic modification within this interval suggests an increase in the frequency of flood events during braided river sedimentation, inhibiting soil development.

Summary and Conclusion

In an ancient system as the Kid area, facies relationships are commonly obscured, and no single facies parameter in isolation is a definitive evidence of a volcanic or sedimentary origin. Exposed on the southern Sinai Peninsula the Tarr sequence in the southern part of the Kid area, is a thick sequence of Late

Proterozoic volcanic and volcanoclastic rocks. During a hiatus in the volcanic activity, and again after volcanism ceased, the volcanic edifice was eroded/ overlapped by ephemeral fluvial processes/deposits. The volcanoclastic rocks are characterized by rapid vertical and lateral facies and petrofacies variation. Compositional analysis of these rocks has revealed that sediment distribution is governed by a variable interplay of volcanic, tectonic and climatic factors.

The sequence in the Tarr area has been divided into three intervals on the basis of the predominant lithosomes in each of the intervals. The lowest interval contains a thick sequence of metamorphosed rocks, volcanic lava flows, pyroclastic deposits and epiclastic rocks including debris flow deposits and sandstones. The last two rock types (debris flow and floodsheets) reflect proximal alluvial fan developed on thick stacking of volcanic and their derivative pyroclastics (volcanic apron environment). The middle interval consists of vertical and lateral stacking of sandstone facies of different grain size, and fining-upwards into mudstones. It reflects deposition of sheetflood and overbank in an inactive flood plain environment. Base level changes became important in controlling incision and expansion of the catchment area (Harvey *et al.*, 1999). The resultant changes operation in the catchment area dramatically increased both sediment and water discharge to the alluvial system, facilitating the changes from alluvial fan to proximal braided river environment of the upper interval. Clast-supported conglomerates are the dominant lithotype in this reach of the river and are abundant in the active channel tract.

Acknowledgement

The author is grateful to Profs. G. Phillips and M.El Sharkawi for their critically reading and constructive comments on the manuscript.

References

- Alexander, J. and Leeder, M.R.** (1987) Active tectonic control on alluvial architecture. In: Etheridge, F.G., Flores, R.M. and Harvey, M.D. (eds) Recent development in fluvial sedimentology. *Soc. Econ. Paleont. & Min. Spec. Publ.*, **39**: 243-252.
- Awad, A.** (1953) Signification morphologique des dépôts lacustres de la Montagne du Sinai central. *Bull. Royal. Soc. Geog.*, **XXV**: 23-28.
- Ayalon, A., Steinitz, G. and Starinsky, A.** (1987) K-Ar and Rb-Sr whole rock ages reset during Pan-African event in the Sinai Peninsula (Ataga area). *Precamb. Res.*, **37**: 191-197.
- Bjerrum, C.J. and Dorsey, R.J.** (1995) Tectonic controls on deposition of Middle Jurassic strata in a retroarc foreland basin, Utah. Idaho trough, western interior, United State. *Tectonics*, **14**: 962-978.
- Blair, T.C.** (1987) Sedimentary processes, vertical stratification sequences, and geomorphology of the Roaring River alluvial, Rocky Mountain National Park Colorado. *J. Sedim.Petrol.*, **57**: 1-18.

- Blair, T.C. and Mc-Pherson, J.G.** (1994) Alluvial fan processes and forms. In: Abrahams, A.D. and Parsons, A.J. (eds.). *Geomorphology of desert environments*. Chapman Hall, 354-402.
- Blasband, B., Brooijmans, P., Dirks, P., Visser, W. and White, S.** (1997) A Pan-African core complex in the Sinai, Egypt. *Geol. Mijnb.*, **76**: 247-266.
- Bonnichsen, B. and Kauffman, D.F.** (1987) Physical features of rhyolite lava flows in the Snake River plain volcanic province, southwestern Idaho. In: Fink, J.H. (ed.). *The emplacement of silicic domes and lava flows*. *Geol.Soc. Am. Spec. Pap.*, **212**: 119-145.
- Branney, M.J. and Kokelaar, P.** (1992) A reappraisal of ignimbrite emplacement: progressive aggradation and particulate to non-particulate transitions during emplacement of high-grade ignimbrite. *Bull. Volcanol.*, **54**: 504-520.
- Bull, W.B.** (1972) Recognition of alluvial fan deposits in the stratigraphic record. In: Rigby, I.K. and Hamblin, W. (eds.). *Recognition of ancient sedimentary environment*. *Soc. Econ. Paleont. Mineral. Spec. Publ.*, **16**: 63-83.
- Bull, S.W.** (1993) Sedimentation and volcanism in an ancient felsic intra-continental rift: the lower Devonian Snowy River volcanics, southeastern Australia. Ph.D. Thesis (unpubl.), Monash Univ.
- Bull, S.W. and Cas, R.A.F.** (2000) Distinguishing base-surge deposits and volcanoclastic fluvial sediments: an ancient example from the lower Devonian Snowy River volcanics, southeastern Australia. *Sedimentology*, **47**: 87-98.
- BVSP-Basaltic volcanism study project** (1981) Basaltic volcanism on the Terrestrial planet, Pergamon Press, Inc., New York, 1286p.
- Calanchi, N., Cattaneo, A., Dinelli, E., Gasparotto, G. and Lucchini, F.** (1998) Tephra layers in Late Quaternary sediments of the central Adriatic sea. *Mar.Geol.*, **149**: 191-209.
- Cas, R.A.F. and Wright, J.V.** (1987) Volcanic successions: Ancient and Modern. *Allen and Unwin, London*, 528 p.
- Cas, R.A.F. and Bushy Spera, C.** (1991) Volcanoclastic sedimentation. *Sediment.Geol.*, **74**, 362 p.
- Chazot, G. and Bertrand, H.** (1995) Genesis of silicic magmas during Tertiary continental rifting in Yemen. *Lithos*, **36**: 69-83.
- Costa, J.E.** (1988) Rheologic, geomorphic and sedimentologic differentiation of water floods hyperconcentrated flows, and debris flows. In: Baker, V.R.; Kochel, R.C. and Patton, C. (eds.). *Flood geomorphology*. Wiley, 113-122.
- Danckwerth, P.A. and Newton, R.C.** (1978) Experimental determination of the spinel peridotite to garnet peridotite reaction in the system MgO-Al₂O₃-SiO₂ in the range 900-1,100°C and Al₂O₃ isopleths of enstatite in the spinel field. *Contrib. Mineral. Petrol.*, **66**: 189-201.
- Dickinson, W.R. and Suczek, C.A.** (1979) Plate tectonics and sandstone compositions. *Am. Ass. Petrol. Geol. Bull.*, **63**: 2164-2182.
- Dickinson, W.R. and Valloni, R.** (1980) Plate settings and provenance of sands in modern ocean basins. *Geol.*, **8**: 82-86.
- Dunne, G.C., Garvey, T.P., Osborne, M., Schneiderei, D., Fritsche, A.E. and Walker, J.D.** (1998) Geology of the Inyo Mountains volcanic complex: Implications for Jurassic paleogeography of the Sierran magmatic arc in eastern California. *GSA Bull.*, **110**: 1376-1397.
- EL-Gaby, S., List, F.K. and Tehrani, R.** (1988) Geology, evolution and metallogenesis of the Pan-African belt in Egypt. In S.North-East African and adjacent areas, *Vieweg, Braunschweig*, 17-68.
- EL-Gaby, S., Khudeir, A.A., Tawab, M.A. and Atalla, R.F.** (1991) The metamorphosed volcano-sedimentary succession of wadi Kid, southeastern Sinai, Egypt. *Annal. Geol. Surv. Egypt*, **XVII**: 19-35.
- Fisher, R.V. and Schmincke, H.U.** (1984) Pyroclastic rocks. *Springer, Berlin*, 472 p.

- Fisher, R.V. and Smith, G.A.** (1991) Volcanism, tectonics and sedimentation. In: Fisher, R.V., and Smith, G.A. (eds.). Sedimentation in volcanic settings: *SEPM (society for sedimentary geology) Spec. Publ.*, **45**: 1-5.
- Fisher, R.V.** (1984) Submarine volcanoclastic rocks. In: Kokelaar, B.P. and Howells, M.F. (eds.). Marginal basin geology. *Geol. Soc. Spec. Publ. Lond.*, **16**: 5-27.
- Furnes, H.J., Shimron, A.E. and Robert, D.** (1985) Geochemistry of Pan-African arc sequence in southeastern Sinai Peninsula and plate tectonic implication. *Precamb. Res.*, **29**: 359-382.
- Gill, J.B.** (1981) Orogenic andesite and plate tectonics. *New York, Springer, Verlag*, 390 p.
- Glass, H.D.** (1958) Clay mineralogy of Pennsylvanian sediments in southern Illinois. In: clays and clay minerals. *Acad. Sci. Natn. Res. Coun. Publ.*, **566**: 227-241.
- Greene, D., Schweickert, R. and Stevens, C.** (1997) The Roberts Mountains allochthon and the western margin of the cordilleran miogeocline in the northern Rilter Range pendant, eastern Sierra Nevada, California. *Geol. Soc. Am. Bull.*, **109**: 1294-1305.
- Halpern, M. and Tristan, N.** (1981) Geochronology of the Arabian-Nubian Shields in southern Israel and Eastern Sinai. *J. Geol.*, **89**: 639-648.
- Hartley, A.J.** (1993) Sedimentological response of an alluvial system to source area tectonism: the Seilao Member of the Late Cretaceous to Eocene purilactis Fm. of northern Chile. *Spec. Publ. Int. Ass. Sediment.*, **17**: 489-500.
- Harvey, A.M.** (1987) Alluvial fan dissection: relationships between morphology and sedimentation. In: Frostick, L. and Red, I. (eds.) Desert sediments: Ancient and Modern. *Geol. Soc. Lond. Spec. Publ.*, **35**: 87-103.
- Harvey, A.M.** (1997) The role of alluvial fans in arid zone fluvial systems. In: Thomas, D.S.G. (ed.). Arid zone geomorphology (2nd edition). *John Wiley & Sons*, 231-260.
- Harvey, A.M., Goy, J.G., Mather, A.M., Silva, P.J., Stokes, M. and Zazo, C.** (1999) Impact of Quaternary sea-level and climate change on coastal alluvial fans in the Cabode Gata ranges, SE Spain. *Geomorphology*, **28**: 1-22.
- Hein, F.J. and Walker, R.G.** (1977) Bar evolution and development of stratification in the gravelly, braided, Kicking Horse River, British Columbia. *Canad. J. Earth Sci.*, **14**: 562-570.
- Huggett, J.M.** (1995) Formation of authigenic illite in Palaeocene mudrocks from the central North Sea: A study by high resolution electron microscopy. *Clays and clay mineral.*, **43**: 682-692.
- Humphreys, B., Smith, S.A. and Strong, G.E.** (1989) Authigenic chlorite in Late Triassic sandstones from the central graben, North Sea. *Clay mineral.*, **24**: 427-444.
- Ingersoll, R.V. and Busby, C.** (1995) Tectonics of sedimentary basins. In: Ingersoll, R.V. and Busby, C. (eds.). Tectonics of sedimentary basins. *Cambridge, Blackwell Science*, 1-52.
- Irvine, T.N. and Barager, W.R.** (1971) A guide to the chemical classification of common volcanic rocks. *Canad. J. Earth Sci.*, **8**: 523-548.
- Issar, A. and Eckstein, Y.** (1969) The lacustrine beds of wadi Feiran, Sinai: their origin and significance. *Israel J. Earth Sci.*, **18**: 21-27.
- Jo, H.R., Rhee, C.W. and Chough, S.K.** (1997) Distinctive characteristic of a stream flow-dominated alluvial fan deposits: Sanghori area, Kyongsang basin (Early Cretaceous), southern Korea. *Sed. Geol.*, **110**: 51-79
- Keller, W.D.** (1970) Environmental aspects of clay minerals. *J. Sed. Petrol.*, **40**: 788-813.
- Keller, W.D.** (1977) Scan electron micrographs of kaolins collected from diverse environments of origin. *Clays and clay mineral.*, **24**: 114-117.
- Kostachuck, R.A., MacDonald, G.M. and Putnam, P.E.** (1986) Depositional processes and alluvial fan drainage basin morphometric relationships near Banff, Alberta, Canada. *Earth Surface Processes and Landforms*, **11**: 471-484.

- Lanson, B., Beaufort, D., Berger, G., Baradat, J. and Lacharpagne, J.C.** (1996) Illitization of diagenetic kaolinite to dickite conversion series: late-stage diagenesis of the lower Permian Rotliegend sandstone reservoir, offshore of the Netherlands. *J. Sed. Res.*, **66**: 501-518.
- Lonsdale, P.** (1975) Sedimentation and tectonic modification of Samoan Archipelagic apron. *Bull. Am. Ass. Petrol. Geol.*, **59**: 780-798.
- Lundberg, N.** (1991) Detrital record of the early central American magmatic arc: petrography of intraoceanic forearc sandstones, Nicoya Peninsula, Costa Rica. *Geol. Soc. Am. Bull.*, **103**: 905-915.
- Machette, M.N.** (1985) Calcic soils of southwestern United States. *Geol. Soc. Am. Spec. Pap.*, **203**: 1-21.
- Massari, F., Mellere, D. and Doglioni,** (1993) Cyclicity in non-marine foreland-basin sedimentary fill: the Messinian conglomerate-bearing succession of the Venetian Alps (Italy). *Spec. Publ. Int. Ass. Sediment.*, **17**: 501-520.
- McKee, E.D., Crosby, E.J. and Berryhill, H.L.** (1967) Flood deposits, Biyou Creek, Colorado. *J. Sed. Petrol.*, **37**: 829-851.
- Miall, A.D.** (1985) Architectural – element analysis: a new method of facies analysis applied to fluvial deposits. *Earth Sci. Rev.*, **22**: 261-308.
- Miall, A.D.** (1996) The geology of fluvial deposits. *Springer-Verlag, Berlin*, 582 p.
- Miall, A.D.** (1978) Lithofacies types and vertical profile models in braided river deposits. A summary. In: Miall, A.D.(ed.) Fluvial sedimentology. *Canad. Soc. Petrol. Geol. Mem.*, **5**: 597-604.
- Moore, I. and KeKelaar, P.** (1998) Tectonically controlled piecemeal caldera collapse: A case study of Glencoe volcano, Scotland. *GSA Bull.*, **110**: 1448-1466.
- Nilsen, T. and Sylvester, A.G.** (1995) Strike-slip basins. In: Busby, C.J. and Ingersoll, R.V. (eds.). Tectonics of sedimentary basins. *Blackwell Science*, 425-457.
- Olson, H. and Larsen, P.H.** (1993) Structural and climatic control on fluvial depositional systems: Devonian, North-East Greenland. *Spec. Publ. Int. Ass. Sed.*, **17**: 401-423.
- Ouchi, S.** (1985) Response of alluvial rivers to slow active tectonic movement. *Geol. Soc. Am. Bull.*, **96**: 504-515.
- Passchier, C.W. and Trouw, R.A.J.** (1996) Microtectonics. *Springer-Verlag, Berlin*, 289 p.
- Peccerillo, A. and Taylor, S.R.** (1976) Geochemistry of upper Cretaceous volcanic rocks from the Pontic chain, northern Turkey. *Bull. Volcanol.*, **39**: 557-569.
- Pearce, J.A.** (1980) Geochemical evidence for the genesis and eruptive settings of lavas from Tethyus ophiolites. *Proceedings of the International ophiolite Symposium, Nicosia, Cyprus*, 261-272.
- Pearce, J.A.** (1982) Trace element characteristics of lava from destructive plate boundaries. In: Throp, R.E. (ed.) Andesite. *John Wiley & Sons LTD., Chichester*, 525-548.
- Priem, H.M., Eyal, M., Heheda, E.H. and Verdurmen, E.Th.** (1984) U-Pb zircon dating in the Precambrian basement of the Arabo-Nubian Shield of the Sinai Peninsula. *A progress report ECOG VIII. Terra Cognita*, **4**: 30-31.
- Pryor, W.A. and Glass, H.D.** (1961) Cretaceous-Tertiary clay mineralogy of the Upper Mississippi embayment. *J. Sed. Petrol.*, **31**: 38-51.
- Retallack, G.J.** (1990) Soils of the past: An introduction to paleopedology. *Unwin*.
- Ritter, J., Miller, J.R., Enzel, Y. and Wells, S.G.** (1995) Reconciling the roles of tectonism and climate in Quaternary alluvial fan evolution. *Geol.*, **23**: 245-248.
- Reymer, A.S., Matthews, A. and Navon, O.** (1984) Pressure-temperature conditions in the wadi Kid metamorphic complex: implications for the Pan-African event in SE Sinai. *Contrib. Mineral. Petrol.*, **85**: 336-345.

- Roser, B.P. and Korsch, R.J.** (1988) Provenance signatures of sandstone-mudstone suites determined using discriminant function analysis of major element data. *Chem. Geol.*, **67**: 119-139.
- Sakran, S.M.** (2000) Fault reactivation and active tectonics in the area between Katherine and Dahab Towns, southern Sinai, Egypt. *Geol. Soc. Egypt.*, **44/1**: 33-53..
- Schwartz, F.W. and Longstaffe, F.J.** (1988) Groundwater and clastic diagenesis. In: Back, W.; Rosenshein, J.S. and Seaber, P.R. (eds.). *Hydrogeology. Geol. Soc. Am.*, **2**: 413-434.
- Shapiro, L. and Brannock, W.W.** (1962) Rapid analysis of silicate, carbonate and phosphate. *US. Geol. Surv. Bull.*, **1144A**: 56p.
- Shimron, A.E.** (1980) Proterozoic island arc volcanism and sedimentation in Sinai. *Precamb. Res.*, **12**: 437-458.
- Shimron, A.E.** (1983) The Tarr complex revisited-Folding, thrusts and mélanges in the southern wadi Kid region, Sinai Peninsula. *Israel J. Earth Sci.*, **32**: 123-148.
- Smith, N.D.** (1974) Sedimentology and bar formation in the upper Kicking Horse river, a braided outwash stream. *J. Geol.*, **82**: 205-223.
- Smith, G.A.** (1986) Coarse-grained nonmarine volcaniclastic sediments: terminology and depositional process. *Geol. Soc. Am. Bull.*, **97**: 1-10.
- Smith, G.A. and Katzman, K.** (1991) Discrimination of Aeolian and pyroclastic surge processes in the generation of cross-bedded tuffs, Jemez Mountains, New Mexico. *Geol.*, **19**: 465-468.
- Stern, R.J.** (1985) The Najd fault system, Saudi Arabia and Egypt. A Late Precambrian rift-related transform system. *Tectonics*, **4**: 497-511.
- Stern, R.J. and Hedge, C.E.** (1985) Geochronologic and isotopic constraints on Late Precambrian crustal evolution in the Eastern Desert of Egypt. *Am. J. Sci.*, **285**: 97-127.
- Stokes, M. and Mather, A.E.** (2000) Response of Plio-Pleistocene alluvial system to tectonically induced base-level changes, Vera Basin, SE Spain. *J. Geol. Soc. Lond.*, **157**: 303-316.
- Surdam, R.C., Boese, S.W. and Crossey, L.J.** (1984) The chemistry of secondary porosity. In: McDonald, D.A. and Surdam, R.C.(eds.). *Clastic diagenesis. Am. Ass. Petrol. Geol. Mem.*, **37**: 127-149.
- Taylor, S.R. and McLennan, S.M.** (1981) The composition and evolution of the continental crust: rare earth elements evidence from sedimentary rocks. *Phil. Trans. R. Soc.*, **301A**: 381-399.
- Treuil, M. and Varet, J.** (1973) Critères volcanologiques, pétrologiques et géochimiques de la genèse de la différenciation des magmas basaltiques: exemple de l'Afar. *Bull. Soc. Geol. France, 7^{em} e serie*, **15**: 401-644.
- Tunbridge, I.P.** (1981) Sandy high-energy flood sedimentation-some criteria for recognition, with an example from the Devonian of SW England. *Sed. Geol.*, **28**: 79-95.
- Weaver, B. and Tarney, J.** (1984) Empirical approach to estimating the composition of continental crust. *Nature*, **310**: 575-657.
- Well, S.G. and Harvey, A.M.** (1987) Sedimentologic and geomorphic variations in storm-generated alluvial fans, Howgill Fells, northwest England. *Geol. Soc. Am. Bull.*, **98**: 182-198.
- Wilson, G.** (1989) Igneous petrogenesis: A Global tectonic approach. *London Unwin Hyman, Boston, Sydney Wellington*, 466 p.
- Williams, P.F. and Rust, B.R.** (1969) The sedimentology of a braided river. *J. Sed. Petrol.*, **39**: 649-679.
- Wright, V.P. and Tucker, M.E.** (1991) Calcretes: an introduction. In: Wright, V.P. and Tucker, M.E. (eds.). *Calcretes. International Ass. Sedimentology Rep. Series*, **2**: 1-22.

Appendix

Analytical Techniques

Major oxides were analyzed using the conventional wet chemistry techniques of Shapiro and Brannock (1962). SiO_2 , TiO_2 , Al_2O_3 and P_2O_5 were analyzed using spectrophotometric techniques. Na_2O and K_2O were analyzed using the flame-photometric techniques. Fe_2O_3 , CaO and MgO were measured by titration. The detected trace elements were determined by X-ray fluorescence (XRF), using Philips X/Unique II with automatic sample charge (Pw 1510). The clay minerals were identified by X-ray diffraction (XRD), using Philips X-ray unit (Pw 3710/31), with Generator (Pw 1830), Scintillation counter (Pw 3020), Cu-target tube (Pw 2233), Ni- filter at 40 kv and 30 mA. All the analyses have been carried out at the laboratories of Egyptian Nuclear Materials Authority (NMA).

تراكم فتات الرواسب البركانية فى منطقة التار

جنوب شرق سيناء - مصر

الشواهد البترولوجية والجيوكيميائية

عزالدين عبد الحكيم خلف

قسم الجيولوجيا ، كلية العلوم ، جامعة القاهرة

الجيزة - جمهورية مصر العربية

المستخلص . تمثل تعقيدات التار الجزء الجنوبى لمجموعة الكيد فى الجزء الجنوبى الشرقى لشبه جزيرة سيناء. ولقد وجد الباحث أن معقد التار يتكون من العديد من الوحدات الطباقية المكونة من البركانيات ورواسب البركانيات الفتاتية الحرارية والرسوبية متداخلة مع الصخور النارية الجوفية والتابعة لحقب البروتيروزويك المتأخر. وقد أوضحت الدراسة أن التتابعات البركانية والرسوبية لمنطقة التار قد مرت بمراحل من عمليات التحول , كما أنها قد تعرضت للقليل من عمليات التشوه. كما أن هذه التتابعات قد تميزت من الناحية الحقلية بكونها ذات تغيرات سحنية كبيرة على المستويين الرأسى والأفقى . وقد أظهر التحليل الظاهرى لهذه التتابعات أن المصدر الأساسى لتلك الصخور هى الصخور البركانية والنارية المتداخلة وذلك اعتمادا على الميزات الصخرية والبتروجرافية لتلك الصخور .

ولقد تمكن الباحث من تقسيم تتابعات التار إلى ثلاث نطاقات طباقية اعتمادا على سحنتها الصخرية المميزة لكل نطاق . أما النطاق السفلى فيتكون من الفتاتيات الحرارية الفلسية المتحولة مع تداخلات من المرمر وأيضا الفتاتيات البركانية ذات التركيب الفلسى والمافى بالإضافة إلى بعض الطبقات المتداخلة ذات التواجد المحدود من الكونجولومرات والحجر الرملى مع بعض الطبقات العدسية من الحجر الطينى . وقد استنتج الباحث أن هذه الصخور الرسوبية قد ترسبت فى بيئات المراوح النهريّة الملازمة فوق البيئة البركانية القديمة . أما النطاق الأوسط فهو

يتكون من حجر رملي كتلى إلى شديد التطبق، خشن إلى متوسط الحبيبات متداخل مع طبقات من الحجر الطيني و طبقات عدسية من صخور بركانية متحولة مافية التركيب . وقد تم ترسيب صخور النطاق الأوسط فى بيئات المراوح النهريه الطرفية . بينما وجد الباحث أن النطاق العلوى لنتابعات التار ذات تركيب يغلب عليه صخور الكونجلومرات المكونة أساسا من الصخور البركانية والنارية الجوفية , ربما يكون قد تم ترسيبها فى بيئات الأنهار الضحلة المصفرة الملازمة فى مجارى السهول النهريه.

ولقد استنتج الباحث أن العمليات التكتونية كانت العامل الأساسى فى عمليات تكوين وتطور الصخور النهريه بمنطقه الدراسة , حيث أن زيادة معاملات الانحدار أثناء عمليات الرفع والانشاء المتتالية أو عن طريق تغير مستوى القاع وأيضا مستوى سطح البحر كان لها التأثير الأكبر فى تغير بيئات الترسيب بين المراوح النهريه الملازمة أو الطرفية إلى بيئات الأنهار المصفرة. كما أن المعدلات العاليه للترسيب قد أدت إلى عدم تكوين التربة بمنطقه الدراسة . وفى النهايه فلقد استنتج الباحث أن هذا التتابع يماثل حافة البركانيات القوسية والتي يمكن أن تكون ? وترسب فى بيئات السهول النهريه الفيضية والمراوح النهريه وأيضا فى بيئات الرواسب الريحية .

طريقة تكرارية لتحديد العمق من متوسط الحيوود المغناطيسية المتبقية من الرتبة الثانية

السيد محمد عبد الرحمن ، طارق محمد العربي و خالد سيد عيسى
قسم الجيوفيزياء ، كلية العلوم ، جامعة القاهرة
الجيزة - جمهورية مصر العربية

المستخلص . نستخدم في هذا البحث طريقة منحنيات النواذف لتحديد العمق للأجسام المدفونة تحت الأرض من متوسط الحيوود المغناطيسية المتبقية من الرتبة الثانية. وتعتمد الطريقة على إيجاد علاقة بين العمق وتشكيل بعض قيم الحيوود عند النقط المميزة للبروفيل. وقد تم تحويل مشكلة إيجاد العمق إلى مشكلة حل معادلة واحدة $E = D(ع)$. ويمكن تطبيق الطريقة ليس فقط على الحيوود المغناطيسية المتبقية الحقيقية ولكن أيضا على الحيوود المغناطيسية الحقلية الناتجة من الأجسام الضحلة والعميقة.

وقد طبقت الطريقة على مجموعات بيانات افتراضية بعضها يحتوى على أخطاء عشوائية وأخرى لا تحتوى على هذه الأخطاء كما تم التأكد من صحة هذه الطريقة بتطبيقها على الحيوود المغناطيسية لجدة رفيعة واقعة ببحيرة بشابو بكندا.